RS-UPM-90-006
DECEMBER 1990

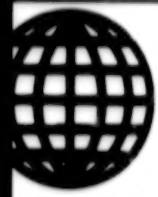

FOREIGN
BROADCAST
INFORMATION
SERVICE

JPRS Report

Science & Technology

USSR: Physics & Mathematics

Science & Technology
USSR: Physics & Mathematics

JPRS-UPM-90-006 14 December 1990

CONTENTS

Nuclear Physics

Optics, Spectroscopy

Plasma Physics

Superconductivity

Differential Equations

Shock Wave Pattern in Transient Glow Discharge Plasma With Ultraviolet Basing

907J0099B Leningrad PISMA V ZHURNAL TEKHNICHESKOY FIZIKI in Russian Vol 16 No 8, 26 Apr 90 pp 30-33

[Article by A. Yu. Gridin, A. I. Klimov, G. I. Mishin, the Engineering Physics Institute imeni A. F. Ioffe at the USSR Academy of Sciences, Leningrad]

[Abstract] This paper continues experimental studies of the shock wave structure in transient glow discharge plasma carried out by Klimov, Mishin, et al. The results from studies on the effect of external ultraviolet radiation of an electric discharge gun on the transverse discharge parameters and the shock wave in the discharge are presented. Experiments were conducted in a special diaphragm shock tube. The gas density in the discharge and behind the shock wave was measured within an 8 percent accuracy by a laser interferometer with a space resolution of at least 1 mm. The interference band shift in the local area behind the shock wave was measured by a collimated FEU-86. The spark gap had a continuous spectrum peaking in the ultraviolet band. A glow discharge with a current density of 15 mA/cm^2 was created in the air at P = 3 torr. The results show that relatively weak ultraviolet radiation at an energy some 25 times less than that is used to create plasma which significantly affects the shock wave parameters in plasma. Since ultraviolet biasing in plasma primarily affects the concentration of electron-excited molecules and electrons due to an additional gas ionization, subsequent studies will be aimed to examine the relationship of these factors to the shock wave structure and perturbation propagation mechanism in plasma. References 4; figures 2.

On Evolutionability of Shock Waves

907J0106A Moscow ZHURNAL EKSPERIMENTALNOY I TEORETICHESKOY FIZIKI in Russian Vol 98 No 1(7), Jul 90 pp 141-145

[Article by S. K. Aslanov, Odessa State University imeni I. I. Mechnikov]

[Abstract] The plane shock wave evolutionability condition, first derived by Landau for a linearized one-dimensional perturbation, is extended to the case of a two-dimensional perturbation which distorts the wave's initial plane surface. A similar analysis is performed for the residual instability interval whereby both branches of the acoustic perturbation are taken into account in plotting the solution. As a result, it is demonstrated that the range, which has been regarded as an area of spontaneous sound emission by the shock, is actually a shock wave non-evolutionability region. This is consistent with a similar conclusion drawn by Kuznetsov. It is established that in the sound emission region, the sound wave actually propagates from the shock. In conclusion, the use of both branches of acoustic perturbation is legitimate, which makes it impossible to close the shock wave instability problem mathematically and attests to an additional plane wave non-evolutionability region. This result is consistent with the conclusions drawn on the basis of the general principle of causality. References 7.

Anomalous Critical Dynamics in Erbium Orthoferrite Low-Temperature Transition

907J0106B Moscow ZHURNAL EKSPERIMENTALNOY I TEORETICHESKOY FIZIKI in Russian Vol 98 No 1(7), Jul 90 pp 334-339

[Article by I. M. Vitebskiy, N. K. Danshin, A. I. Izotov, M. A. Sdvizhkov, L. T. Tsymbal, Donetsk Engineering Physics Institute at the Ukrainian Academy of Sciences]

[Abstract] Critical behavior of the acoustic and magnetic resonance properties of the low-temperature phase transition in erbium orthoferrite is examined experimentally in a wide-band microwave spectrometer and ultrasonic spectrometer at practically liquid nitrogen temperatures. Measurement samples were made from single crystals grown by floating zone melting with radiant heating. A sharp asymmetry of acoustic and magnetic resonance plots, relative to the critical point, and an exceptionally high acoustic anomaly near the liquid nitrogen temperature was observed, as well as the fact that the softening magnetoresonance mode reached a minimum long before the critical point and then remained constant up to the liquid nitrogen temperature. The greatest acoustic anomalies were also observed in that region. Conclusively, an unusual character of $ErFeO_3$ dynamic properties in the vicinity of the critical point is primarily due to the combined nature of the corresponding phase transition whereby the order of a rare earth subsystem is accompanied by a reordering of the iron sublattice magnetization. References 8; figures 3.

Magnetoacoustic Oscillations of Longitudinal Sound Harmonics in Metals

907J0106C Moscow ZHURNAL EKSPERIMENTALNOY I TEORETICHESKOY FIZIKI in Russian Vol 98 No 1(7), Jul 90 pp 340-348

[Article by V. A. Burdov, V. Ya. Demikhovskiy, Gorkiy State University imeni N. I. Lobachevskiy]

[Abstract] Longitudinal sound wave harmonics generation in a strong magnetic field with magnetoacoustic oscillations of the sound absorptance is analyzed. A longitudinal sound wave propagating at an angle φ to the static magnetic field direction is examined. It is found that the amplitudes of higher harmonics oscillate with magnetic field variations and the period of oscillations coincides with that of magnetoacoustic oscillations of the sound absorptance. Oscillations develop when groups of resonance electrons traverse either the boundary points or the extremal cross section. Both cases of oscillations are examined. It is found that the harmonics amplitude increases with distance from the sample boundary and depends on the fundamental wave amplitude; it also decreases rather slowly with an

increase in the number of harmonics. The conclusion is drawn that the behavior of the magnetoacoustic amplitude harmonic oscillation modes remains valid when angles φ are not too close to $\pi/2$; it is also necessary that cyclotron resonances be spaced sufficiently far from each other. References 6; figures 1; tables 1.

Multifractal Structure of Developed Hydrodynamic Turbulence and Kolmogorov's Third Hypothesis

907J0106D Moscow ZHURNAL EKSPERIMENTALNOY I TEORETICHESKOY FIZIKI in Russian Vol 98 No 1(7), Jul 90 pp 146-161

[Article by A. Yu. Turygin, V. R. Chechetkin, Atomic Energy Institute imeni I. V. Kurchatov]

[Abstract] Intermittency effects, caused by the energy dissipation rate fluctuations, are examined. These effects are manifested in the appearance of a sharply inhomogeneous spatial structure of the energy dissipation field. It is shown that the use of the bounded lognormal distribution, instead of the unbounded Kolmogorov Obukhov distribution, makes it possible to avoid major difficulties related to the use of unbounded distributions and attain results consistent with experimental data. In a first approximation, the mechanism based on a nonlinear interaction of long wave and inertial turbulent pulsations yields intermittency characteristics which are close to those observed. The effect of the developed hydrodynamic turbulence's multifractal structure is considered with respect to the passive impurity distribution intermittency. Available experimental data are consistent only with two models: the two-scale Cantor approximation and bounded lognormal distribution. To explain the more singular character of the passive impurity concentration distribution, the simplest doubly-random cascade model was used. The authors are grateful to A. A. Vedenov and A. L. Chernyakov for discussing the results. References 43: 13 Russian, 30 Western; figures 9.

Spontaneous Loss of Scale Invariance in Fractal Turbulence

907J0106E Moscow ZHURNAL EKSPERIMENTALNOY I TEORETICHESKOY FIZIKI in Russian Vol 98 No 1(7), Jul 90 pp 162-167

[Article by A. G. Bershadskiy, Makeyevka Construction Engineering Institute]

[Abstract] Scale invariance is a property of developed turbulence in a certain range of scales. Since scaling in this case is due to the inertial character of motion, this range is also referred to as the inertial range. Yet, scaling breaks up near the range boundaries. The behavior of turbulence near the scale invariance range boundaries is analyzed; more specifically, the behavior of the spectral energy density of fractal turbulence near the small-scale (shortwave) scaling range boundary is examined and its variation law is derived. It is established that the results predicted by this law are consistent with experimental data of various authors. The author is grateful to G. I. Barenblatt for useful remarks. References 10: 4 Russian, 6 Western; figures 4.

Superfluid Bose Liquid With Intense Boson Pair Condensate

907J0106F Moscow ZHURNAL EKSPERIMENTALNOY I TEORETICHESKOY FIZIKI in Russian Vol 98 No 1(7), Jul 90 pp 178-195

[Article by Yu. A. Nepomnyashchiy, E. A. Pashitskiy, Physics Institute at the Ukrainian Academy of Sciences]

[Abstract] It is shown that the combination of a weak single-particle condensate and an intense pair condensate leads to an instability which results in the possible disappearance of the single-particle condensate while the pair condensate is retained or even enhanced. Qualitative patterns of the state of pair condensate, without the single-particle condensate, which are manifested in the effective condensate structure and in the character of hydrodynamics as well as restrictions on the "hybridization" of excitations and their spectra are analyzed. It is shown that single-particle condensates disappear by means of a phase transition of the first kind and an abrupt appearance of a gap in the single-particle spectrum. An exact diagram equation of the energy components proper is examined. Peculiarities of the restructured state of Bose-liquid without the single-particle condensate are investigated. The results are discussed from the viewpoint of their applicability to describing other Bose-liquids, such as liquid ^{4}H, excitons in semiconductors, and bipolarons in ionic crystals. In conclusion, the structure of the superfluid state of Bose-liquid depends on the polarity of the paired interaction among the particles: given a repulsion, the superfluid effective condensate is determined by the the single-particle condensate as well as higher condensates. In the case of a sufficiently strong attraction, the superfluid component has a "paired" origin and consists of coupled "Cooper pairs" with a large radius, leading to a gap in the single-particle boson spectrum, certain heat capacity anomalities, a doubling of the velocity circulation quantum, and an exponential rather than power-law character of the pair correlations asymptotics. References 47: 25 Russian, 22 Western; figures 3.

UDC 621.373:535

New Lasing Channels in Tm^{3+} Ion

907J0019A Leningrad OPTIKA I SPEKTROSKOPIYA in Russian Vol 68 No 2, Feb 90 pp 282-283

[Article by B.M. Antinenko, S.P. Voronin, and T.A. Privalova]

[Abstract] An experiment has confirmed the possibility of visible and infrared lasing transitions from the $^1G_4$ level in the Tm^{3+} ion upon selective excitation of Yb^{3+} sensitizer ions in $BaYb_2F_8$:Tm^{3+} crystals by a Nd-laser. Earlier studies and theoretical analysis of energy transfer in such crystals has already revealed that intense excitation causes the $^3H_4$ level to become the one most likely to be lasing in a crystal with 1-2 atom.% Tm and the $^1G_4$ level to become the one with the largest population in a crystal with only 0.2-0.3 at.%. Tm. The measured emission spectra and the recorded absorption spectra of a $BaYb_2F_8$:(0.2 at.% Tm) crystal in an optical cavity between two mirrors indicate that the $^1G_4 \rightarrow {}^3F_4$ is attended by emission of 648 nm radiation without resonance losses and the $^1G_4 \rightarrow {}^3F_3$ transition is attended by emission of 1,580 nm radiation without counterabsorption.

UDC 621.373.826

Effect of Heating on Efficiency of Excimer-Pumped Pulsed Dye Lasers

907J0039A Tallinn IZVESTIYA AKADEMII NAUK ESTONII: FIZKA, MATEMATIKA Vol 39 No 1, Jan-Mar 90 pp 52-55

[Article by Yevgeniy Berik and Vladimir Davydenko, Institute of Physics, ESSR Academy of Sciences]

[Abstract] Pumping of visible and infrared dye lasers with ultraviolet excimer electric-discharge lasers is considered. A major problem with this is the wide Stokes shift, and consequently much larger amount of heat per photon injected into the active medium than during pumping with a YAG laser or, in the case of transverse pumping, with a nitrogen laser. Therefore, an experimental study of transverse pumping with an excimer laser was made concerning the effect of optical inhomogeneities produced in the active medium by intense heating on the efficiency of a pulsed dye laser. Such a laser with rhodamine 6G or another class VL-10 dye as active medium in a 20 mm long cell was placed inside a 245 mm long optical cavity between an echelette diffraction grating with 600 grooves/mm and a plane exit mirror with an R = 0.04 reflection coefficient. Between the cell and the diffraction grating was placed a 40x beam expander, the reflection coefficient per expander-grating pass being r = 0.12 for 600 nm radiation. As source of pumping radiation was selected, an ELI-3 electric-discharge laser delivered pulses of up to 40 mJ energy at a repetition rate of 10 Hz. Pumping pulses from the EI 1-3 laser and output pulses from the dye laser was recorded on an S8-13 stroboscopic oscillograph, aided by two photoelectric switches. The average emission power of both lasers was measured with an IMO-2N calorimeter. These measurements have yielded the relation between energy in an output pulse and energy in a pumping pulse, the relation being linear up to 5 mJ pumping energy with a corresponding 0.6 mJ output energy (15 percent efficiency). As the pumping energy was further increased, the output energy increased less than linearly corresponding to an increasing drop of laser efficiency. The waveform of output pulses also changed, the leading edge shifting slightly and the peak power remaining proportional to the pumping energy, but the trailing edge was cut and the pulse duration thus became shorter. The results of the experiment are interpreted in terms of the stability criterion for an optical cavity, the analysis being based on the model of a laser and a diverging lens inside the optical cavity and the theoretical dependence of the stability criterion on the focal length of that lens. This lowering of the laser efficiency as the pumping energy increases is, according to this model, attributable to heating which induces a thermal lens inside the cavity and thus destabilizes the latter so that the emission time is shortened. Article was presented by P. Saari. Figures 4, references 11.

UDC 621.373.826

Periodically Pulsed Nd-Glass Solid-State Power Laser With Tabular Active Medium

90J0041A Moscow KVANTOVAYA ELEKTRONIKA in Russian Vol 17 No 4, Apr 90 pp 398-403

[Article by M.A. Borik, P.V. Gorbunov, Yu.K. Danileyko, B.I. Denker, A.D. Ivanov, N.N. Ilichev, A.V. Larikov, T.P. Lebedeva, G.V. Maksimova, V.V. Motsartov, A.G. Musatov, V.V. Osiko, and P.P. Pashinin, Institute of General Physics, USSR Academy of Sciences, Moscow]

[Abstract] The performance of periodically pulsed solid-state power lasers for treatment of structural materials is examined. Of particular interest were recently developed lasers with Nd-doped phosphate glass as active medium capable of delivering an average pulse power of over 1 kW at repetition rates of up 100 Hz. The key feature of these lasers is an approximately 0.6 cm thick large tabular, rather than cylindrical, active element. The design of such an active element involves an analysis of thermal stresses and estimation of the specific power output, i.e., power evolving within the upper laser level of active Nd ions per unit area of the lateral plate surface. Taken into account is multiple passage of narrow-band pumping radiation through the active element and attendant absorption of that radiation by it; the total specific power being obtained by integration over the absorption spectrum of the active medium and matched with the emission spectrum of the pumping source (lamp). What has been designed, on the basis of such an

analysis, is a thin tabular active element of K-Na phosphate glass with a high Nd concentration, 8.10^{20}ions/cm^3, this plate being 0.42 cm thick and 15 cm long. This active element was pumped, symmetrically, by two rows of eight independently energized INP-5/90 flash lamps inside an open luminaire-reflector with an electrolytically deposited and then polished silver surface coating. With a pumping power of 9 kW, this laser delivered a maximum average pulse power of 180 W at repetition rates of 5 and 10 Hz. Figures 3; references 20.

UDC 621.373.826

New High-Intensity Bands in Nonlinear Absorption and Multiphoton Dissociation Spectrum of SiH_4 Within 11-μm Emission Band of $^{13}C^{16}O_2$ Isotope Laser

907J0041B Moscow KVANTOVAYA ELEKTRONIKA in Russian Vol 17 No 4, Apr 90 pp 507-509

[Article by M.S. Dzhidzhoyev, S.V. Kamayev, V.K. Popov, and A.V. Chugunov, Moscow State University imeni M.V. Lomonosov]

[Abstract] The nonlinear-absorption spectrum of monosilane SiH_4 within the 880-905 cm^{-1} range was studied, the object was to increase the efficiency of vibrational excitation by single-frequency and two-frequency infrared laser radiation and, to not only lower the threshold for multiphoton dissociation of a monosilane molecule under low pressure, but also to increase the yield of such a dissociation. The nonlinear absorption spectrum of monosilane, including a 927-960 cm^{-1} band, was measured with an optoacoustic detector during irradiation of a specimen with unfocused infrared light under a pressure of approximately 1 mm Hg. Radiation, corresponding to the 11P(20) line of a $^{13}C^{16}O_2$ laser, was found to have been absorbed at a rate five times higher than radiation corresponding to the most intense 10P(36) line of a $^{12}C^{16}O_2$ laser. Shifting the excitation toward longer waves has subsequently revealed three new lines of a $^{13}C^{16}O_2$-isotope laser: 11P(14), 11P(20), 11P(28). Accordingly, it was possible in this way to increase the efficiency of excitation and the yield of multiphoton dissociation and also lower the threshold for such a dissociation. The intensity of luminescence of the dissociation products, proportional to the dissociation rate, was found to be linearly dependent on the pressure over the 0.1-10 mm Hg range during excitation at both 10P(38) and 10P(24) lines. This indicates a monomolecular, collisionless dissociation under these conditions. Under two-frequency infrared excitation of monosilane with a low energy density of 0.01-0.02 J/cm^2 and under a pressure of 1 mm Hg, the detector signal was simply the sum of signals picked up upon excitation by each of the two lasers independently. Under two-frequency excitation of monosilane with a high energy density of 100 J/cm^2 or more, the higher yield of monosilane multiphoton dissociation, as well as the luminescence signal, were found to depend strongly on both the frequency difference and on the time interval between excitation pulses from the two lasers. Figures 3; references 7.

Action of Low-Intensity Laser Radiation on Biological Tissues

907J0044A Leningrad PISMA V ZHURNAL TEKHNICHESKOY FIZIKI in Russian Vol 16 No 6, 26 Mar 90 pp 46-49

[Article by O.Yu. Voronina, M.A Kaplan, and V.A. Stepanov]

[Abstract] While action of laser radiation on biological tissues is most commonly associated with activation of photoreactions in them, this does not explain why different photoreactions lead to the same stimulating action of 0.4-0.6 μm laser radiation or of 0.8-1.0 μm laser radiation and thus, within the spectral range, void of absorption resonances in such tissues. Therefore a different interpretation is proposed, namely that action of laser radiation produces a nonuniform temperature distribution in biological tissues owing to a nonuniform distribution of absorption centers in them. Inasmuch as the pattern of this temperature nonuniformity depends largely on both wavelength and spectral density of the incident radiation, it is theoretically demonstrated that this nonuniformity can cause large deformations of the cell membrane. Considering that protoplasm layers act, not only as barriers between the cell content and the ambient medium but also, as highly selective filters which sustain the difference of ion (K, Na) concentrations on both sides. The action of laser radiation is interpreted in terms of buildup of osmotic pressure due to concentration or temperature imbalance. The phenomenon is analyzed according to the theory of membranes and the results of this analysis are applied to conditions simulating therapeutic treatment with a pulsed low-intensity (1W/cm^2)He-Ne laser. References 6.

Burst-Like Emission Initiated by Laser at Metal-Plasma Interface

907J0044B Leningrad PISMA V ZHURNAL TEKHNICHESKOY FIZIKI in Russian Vol 16 No 6, 26 Mar 90 pp 88-92

[Article by N.K. Berezhetskaya, V.A. Kopyev, and I.A. Kossyy, Institute of General Physics, USSR Academy of Sciences, Moscow]

[Abstract] An experimental study has established the feasibility of initiating burst-like emission at a metal-plasma interface by means of a laser beam and subsequently forming a "unipolar" arc. Dense and hot high potential corona plasmas with a lifetime of 10-100 μs, an electron temperature reaching 200 eV, and an electric potential reaching 2 kV, were generated inside a vacuum chamber by a high-power microwave radiation beam impinging on a dielectric or metal-dielectric target and

interacting with the ionized material in the "resonance" mode. A cylindrical aluminum electrode was inserted into the plasma. The formation of an explosive emission center, the attendant flow of a quasi-steady electron current in the electrode-plasma-wall-electrode circuit upon application of a microwave radiation pulse, and 2 μs later a laser radiation pulse, were monitored on oscillograms, the arc having been localized at the site on the metal electrode surface most convenient for measurements and recording. Figures 3; references 8.

Effect of Low-Frequency Modes of Fluctuating Field on Soliton Dynamics

907J0044C Leningrad PISMA V ZHURNAL TEKHNICHESKOY FIZIKI in Russian Vol 16 No 6, 26 Mar 90 pp 53-56

[Article by V.M. Loginov]

[Abstract] Propagation of a soliton through a medium whose properties fluctuate randomly in space and time is analyzed; the effect of the various fluctuation modes is important from the standpoint of data transmission over nonlinear lines. On the basis of a soliton description by hyperbolic functions and for fluctuations without a zeroth-mode which produce a Gaussian white noise, it is demonstrated by the asymptotic behavior of the solution to the equation for the mean of a sufficiently smooth function that the lowest-frequency fluctuation modes destabilize the soliton evolution and diffuse a soliton. References 6.

UDC 535.37

Sc-Er Garnets With Chromium as Active Media for 1.5-μm Lasers

907J0067A Minsk ZHURNAL PTRIKLADNOY SPEKTROSKOPII in Russian Vol 52 No 4, Apr 90 pp 550-554

[Article by V.A. Smirnov, A.I. Talybov, and I.A. Shcherbakov, Institute of General Physics, USSR Academy of Sciences, Moscow]

[Abstract] An experimental study of three scandium garnets (Gd-Sc-Al, Y-Sc-Ga, Y-Sc-Al) doped with Er^{3+} or Yb^{3+} and Er^{3+} ions, was made. Cr^{3+} ions were added to activate luminescence of those trivalent rare-earth ions in such garnets, and the latter was then tested for efficiency as pulsed infrared lasers. Measurements have yielded the luminescence spectra of Cr, Yb, Er ions and the lifetime of their excited state in each of the three different garnets, the C_{DA} microparameter of Cr → Yb and Cr → Er energy transfers during respective radiationless interactions as well as the quantum yield of Cr-ion → Yb-ion → Er-ion and Cr-ion → Er-ion (no Yb) energy transfers. From the luminescence and absorption spectra of Er ions at room temperature was determined the spectrum of net gain or efficiency of the $^4I_{13/2}$–$^4I_{15/2}$ transition in these ions at room temperature. From the luminescence and absorption spectra of Yb ions at 77 K temperature were determined, not only schematically, the Stark splits of the two $^2F_{7/2}$ and $^2F_{5/2}$ levels in these ions, but also very reliably, the wavelengths of the three bright phononless A, D, D' lines. On the basis of these data, a Gd-Sc-Al garnet was found to be the best active medium for a 1.5-μm laser and the quantum yield of Cr-ion → Er-ion energy transfer populating the $^4I_{13/2}$ level in Er ions is higher than that of the Cr-ion → Yb-ion → Er-ion energy transfer. The choice of a Gd-Sc-Al:(Cr^{3+},Er^{3+}) laser was validated by an experiment with two identical Gd-Sc-Al garnet crystals containing 3.10^{20}cm^{-3} Cr ions and 7.10^{19} cm^{-3} Er ions each, and one also containing 10^{21} Yb ions. The intensity of luminescence of Er ions in the garnet crystal, without Yb ions, was five times higher than in the one with them. The authors thank Ye.V. Zharikov and A.L. Lenisov for supplying the garnets. Figures 3; references 13.

Acceleration of Electrons by Intense Laser Radiation in Constant Magnetic Field

907J0073C Moscow ZHURNAL EKSPERIMENTALNOY I TEORETICHESKOY FIZIKI in Russian Vol 97 No 5, May 90 pp 1498-1509

[Article by V.V. Apollonov, A.I. Artemyev, Yu.I. Kalachev, A.G. Suzdaltsev, A.M. Prokhorov, and M.V. Fedorov, Institute of General Physics, USSR Academy of Sciences]

[Abstract] A new method is proposed for acceleration of electrons by laser radiation, efficient schemes devoid of explicit resonance modes being devised which may be adequate for, and therefore adaptable to, cyclic acceleration process characteristics. The theory of this method is demonstrated on a model electron moving in a constant magnetic field, then add a laser radiation field polarized in the transverse plane and focused on the electron. The acceleration of an electron in a transverse magnetic field is calculated according to the first-order perturbation theory, then in the square-law approximation for a slow electron, and then for a fast electron in additional quasi-stationary crossed magnetic and electric fields. Numerical estimates are followed by consideration of an electron moving in a longitudinal magnetic field and calculation of its acceleration by a laser radiation field according to the second-order perturbation theory. Figures 8; references 17.

Partial Conservation of Axial Current and Nuclear Shielding of Interaction Involving High-Energy Neutrinos

907J0073D Moscow ZHURNAL EKSPERIMENTALNOY I TEORETICHESKOY FIZIKI in Russian Vol 97 No 5, May 90 pp 1418-1428

[Article by B.Z. Kopeliovich, Joint Institute of Nuclear Research]

[Abstract] Nuclear shielding of interactions is shown to follow a different nontrivial pattern for interactions involving neutrinos as compared to interactions involving photons, this being demonstrated by partial conservation of the axial current in the $\nu T \to lF$ interaction (ν-neutrino, T-target, l-any lepton including another neutrino, F-final hadronic state) and specifically, the $\nu\nu$ interaction with the total integral cross-section $\Delta N/\Delta Q^2$ events/GeV^2 depending on Q^2 (Q-momentum transferred from neutrino to lepton or from one neutrino to the other). After the total cross-section for scattering of neutrinos by nuclei has been corrected, so as to take into account inelastic collisions as well as other factors and the results have been compared with experimental data, it becomes evident that shielding is caused not by virtual emission of high-energy neutrinos, but rather by real diffractional production of pions by neutrino-nucleon interactions and that the shielding effect saturates when the neutrino energy is still rather low. The author thanks V. Venus and other participants in the WA59 Collaboration for discussions which provided a stimulus for writing this article, also B.G. Zakharov, Ye M. Levin, N.N. Nikolayev, and B.M. Pontecoro for helpful discussions. Figures 9; references 21.

UDC 681.7.068.4

New Method of Producing Fiber Optic Waveguides Doped With Rare Earth Elements

907J0098A Moscow KVANTOVAYA ELEKTRONIKA in Russian Vol 17 No 7, Jul 90 pp 813-814

[Article by A. A. Abramov, M. M. Bubnov, A. Ye Voronkov, A. N. Guryanov, G. G. Devyatykh, Ye. M Dianov, Yu. B. Zverev, S. V. Ignatyev, N. S. Karpychev, S. M. Mazavin, A. M. Prokhorov, General Physics Institute at the USSR Academy of Sciences, Moscow, and High-Purity Compounds Institute at the USSR Academy of Sciences, Gorkiy]

[Abstract] The results of an examination of optical characteristics of activated fiber optic waveguides produced by a modified vapor phase axial deposition (VAD) method are presented. The blanks were doped directly during the deposition by injecting volatile organometallic compounds of the corresponding rare earth elements into the oxydric torch flame. Impurities were removed from source organometallic compounds by fractional distillation, whereby the transition group concentration following the purification did not exceed 10^{-7} percent. Erbium ion concentration in the single and multimode fiber optic waveguides thus produced, varied between 1.6×10^{-3} percent and 1.0×10^{-2} percent although additional experiments show that the degree of doping can be increased even further. Thus, the conclusion can be drawn that the technology developed on the basis of the VAD method will make it possible to produce single and multimode activated fiber optic waveguides with low losses doped with various rare earth elements. Compared to previous methods, the proposed technology makes it possible to avoid impregnating porous blanks with salts of rare earth elements and is especially useful for doping simultaneously with several coactivators. References 9; 9 Western, figures 2.

UDC 621.373.826

Optically Pumped Free Electron X-Ray Laser: A Two-Level Quantum Oscillator With Completely Inverted Active Medium

907J0098B Moscow KVANTOVAYA ELEKTRONIKA in Russian Vol 17 No 7, Jul 90 pp 815-816

[Article by E. M. Belenov, S. V. Grigoryev, A. V Nazarkin, I. V. Smetanin, Physics Institute imeni P. N Lebedev at the USSR Academy of Sciences, Moscow]

[Abstract] Classical equations describing the free electron laser gain are valid when the stimulated electron beam emission (absorption) line width considerably exceeds the generated field quantum. A situation where an increase in the stimulated field frequency has an opposite effect is examined. In this case, the electron energy variation in the field can only be described by quantum equations of transfers between two energy levels. The threshold of the onset of quantum effects falls within the X-ray band. Thus, an optically pumped two-level free electron laser can serve as an efficient device for attaining coherent X-ray emission. It can operate with a 100 percent inversion utilization per pass, and with respect to the energy parameters, it is not inferior to undulatory (noncoherent) X-ray sources and does not call for using GeV electron beams with accumulator rings. References 7; 4 Russian, 3 Western; figures 1.

UDC 621.373.826.038.825.2

Compact Laser With Stimulated Brillouin Scattering Mirror Operating at Pulse Repetition Frequencies of Up to 150 Hz

907J0098C Moscow KVANTOVAYA ELEKTRONIKA in Russian Vol 17 No 7, Jul 90 pp 851-853

[Article by B. I. Denker, I. Kertesz, P. P. Pashinin, V. S. Sidorin, Ye. I. Shklovskiy, General Physics Institute at the USSR Academy of Sciences, Moscow]

[Abstract] A version of a laser-oscillator with an SBS mirror activated by its own seed emission suggested by Pashinin and Shklovskiy was examined. It differed from

the original in that the auxiliary resonator was rather short (approximately 30 cm). A YAG:Nd^{3+} active element was used in the experiment. $GeCl_4$, $TiCl_4$, CCl_4, and acetone were used as SBS active media. The active element was pumped by one or two synchronized power supply units at pulse repetition frequencies from 0 to 150 Hz and an energy of 25 J. The effect of beam parameters and the medium on the SBS mirror cutoff frequency, as well as the effect of thermal distortions in the active medium on the lasing efficiency, was examined. The authors are grateful to K. Yu. Abbakumov for making the BPL33/75U unit synchronizing circuits. References 7: 5 Russian, 2 Western; figures 3.

UDC 621.373.826.038.825.2

Tunable Picosecond LiF:F_2^+ Oscillator Synchronously Pumped by Second Harmonic Pulses of $KGd(WO_4)_2:Nd^{3+}$ Laser

907J0098D Moscow KVANTOVAYA ELEKTRONIKA in Russian Vol 17 No 7, Jul 90 pp 867-868

[Article by S. R. Grefenshteyn, M. A. Kharchenko, V. V. Shuvalov, Moscow State University imeni M. V. Lomonosov]

[Abstract] Prospects of using LiF:F_2^+ crystals in tunable picosecond oscillators synchronously pumped by second harmonic pulses of a $KGd(WO_4)_2:Nd^{3+}$ (PGT:Nd^{3+}) laser are examined. Interest in this subject arose due to the fact that LiF:F_2^+ crystals are the only active medium whose gain covers the 0.85-1.05 μm band. Beveled, bleached 60 mm long rods of PGT:Nd^{3+} with a 4 and 5 mm diameter, respectively, were used as active elements. A 4 cm long KDP crystal was used to translate radiation to the second harmonic and heterodyne frequencies. Trains of 10-15 pulses were emitted; stimulated emission of bandwidth-limited pulses was realized in the 0.98-1.00 μm band, peaking at 0.93 μm. An analysis of the energy, spectral, and time response of the tunable synchronously pumped picosecond oscillator indicate that such designs can be widely used in various fields of science and engineering. References 5; figures 2.

UDC 621.373.826

Wave Transformation in Beams With Variable Cross Section

907J0098e Moscow KVANTOVAYA ELEKTRONIKA in Russian Vol 17 No 7, Jul 90 pp 920-924

[Article by A. P. Vasin, V. F. Yefimkov, I. G. Zubarev, A. R. Petrukhin, V. B. Sobolev, Physics Institute imeni P. N. Lebedev at the USSR Academy of Sciences, Moscow]

[Abstract] Attempts to improve the performance of SS amplifiers and hypersonic OPC mirrors by using variable cross section beams prompted an examination of the interaction of SS waves, allowing for the variable cross section beam saturation both in the external signal amplification and four-wave mixing modes. The beam energy and shape, interacting in the mixer and long-range distribution, were measured in the experiments. Calculation results show that the reflection factor of the divergent beam exceed that of the convergent one. It is also shown that in the external signal SS amplification mode, an infinite set of geometric shapes of the pump beam with the same equivalent area are similar with respect to the pump conversion to the amplified emission. In the hypersonic OPC mirror design where four-wave mixing with a strong signal wave occurs over the entire signal beam length, the reflection factor can be increased by using a signal beam whose cross section area increases along the signal movement direction. References 6: 4 Russian, 2 Western; figures 3.

UDC 539.374.02+574.4

Structure-Analytical Theory of Strength in Multilevel Formulation

907J0025A Kiev IZVESTIYA VYSSHIKH UCHEBNYKH ZAVEDENIY: FIZIKA in Russian Vol 33 No 2, Feb 90 pp 121-139

[Article by V.A. Likhayev and V.G. Malinin, Leningrad State University]

[Abstract] Mathematical models of deformation and fracture processes are constructed on the basis of a multilevel structure with interactions. The concept of two structural levels is introduced into the theory of plasticity for crystals slipping under a mechanical load. The principal problem here is the selection of the elementary lowest, or first level, as structural scale so that an event of plastic deformation in one site does not depend on analogous, and other events, elsewhere in the crystal. From the standpoint of physical interpretation, this level should be invariant with respect to the loading mode. From the standpoint of engineering strength analysis, this level should be as large-scale as possible. The second structural level must be sufficiently high for identifying the properties of the crystal as a whole, which requires both statistical and directional averaging of microstrains into the macrostrain and taking into account the rather strong interaction of different regions having the same characteristic volume. The relation between first and second levels having been established, tensor calculus and laws of evolution are applied to orientation analysis of microstresses, with the aid of two distribution functions representing the structure statistics and the directional pattern of slip planes respectively. A connectedness diagram is constructed for deformation by slip according to this multilevel model, and with its aid, the relation between the parameters of this theory and the physical processes which control plastic flow is established. The concept of three structural levels is next introduced into the theory of defectiveness and fracture. A microcrack is selected as the lowest, or first, structural level here, considering that a microcrack can nucleate only when the integral shear strain intensity in a slip plane has reached its critical level and when the force criterion for crack opening is satisfied. A set of three microdefectiveness parameters are defined at this level, two of them, π^c and π^b associated with the mechanical mechanism of cut cracking and breakaway cracking respectively, and the third one, π^t associated with the thermal fluctuation mechanism of cracking. Growth of microcracks, rather than their mere appearance, is the prerequisite for fracture; additional force or energy criteria pertaining to their propagation are needed for strength analysis with the aid of microdefectiveness vectors characterizing cut and breakaway cracks. Selection of the second or intermediate structural level requires both statistical and directional averaging of all three microdefectiveness parameters, which leads to a new microdefectiveness parameter that represents the integral microdefectiveness within the characteristic volume. Stresses and strains must be renormalized to account for nonuniformity of their distribution owing to discontinuities, the concentration of which is characterized by that integral microdefectiveness parameter, and it also must account for inelastic deformation as well as for thermal expansion. Partitioning into separate segments is then selected as the upper, or third, structural level. A connectedness diagram is constructed now for defectiveness of a crystal as a whole. Use of the structural multilevel formalism for an evaluation of functional mechanical properties of crystalline materials with shape memory is demonstrated on martensitic transformations of the first kind, where growth of the martensitic phase depends on both temperature and pressure according to the universal Clausius-Clapeyron law. Figures 3; references 62.

Dielectric Relaxation in Nonhomogeneous Medium in Model of Random Fractals

907J0028A Leningrad ZHURNAL TEKHNICHESKOY FIZIKI in Russian Vol 60 No 2, Feb 90 pp 45-53

[Article by R.R. Nigmatullin and N.N. Sutugin, Kazan State University imeni V.I. Ulyanov-Lenin]

[Abstract] The concept of fractals is extended from regular to random ones for description of a nonhomogeneous medium and analysis of dielectric relaxation in such a medium which, according to the Debye relaxation of an electric dipole, manifests itself by a decrease of the depolarization current. The model of random fractals describes a nonhomogeneous medium as an ensemble of fractals with random scales η, ranging from scale λ of the smallest fractal that can form here to the characteristic length equal to scale Λ of the largest fractal. The average volume of a fractal of a given scale η is, in the case of a continuous distribution of scales over this (λ,Λ) range, equal to the integral over this range of its actual volume multiplied by the probability $W(\eta)$ of finding a fractal of that scale within the $[\eta, \eta+d\eta]$ interval. The probability of a function $W(\eta)$ must be such that its normalization to unity and subsequent averaging of the fractal volume by integration will not break the self-similarity of the medium's structure. A probability function described by the expression $W(\eta) = (1 + \alpha)/\Lambda(1 - \mu^{1+\alpha}).(\lambda/\Lambda)^{\alpha}$ where $\alpha = 1/D$ (D-logarithmic mean fractal dimensionality) and $\mu = \lambda/\Lambda$ satisfies the principle of statistical self-similarity within certain ranges of α and μ. A description of dielectric relaxation in terms of this statistical fractal model yields new expressions for the depolarization current and for the dielectric loss, also for the frequency dependence of the dielectric permittivity, which take into account the porosity of a fractal medium. They also explain the "universal" response of nonhomogeneous solid dielectrics regardless of their physical structure and chemical bond between molecules with any form of polarization. Figures 3; tables 2; references 14.

Feasiblity of Using Optical Transition Radiation for Diagnostic Testing of Proton Beams From U-20 Accelerators and for Nondestructive Inspection Apparatus

907J0028B Leningrad ZHURNAL TEKHNICHESKOY FIZIKI in Russian Vol 60 No 2, Feb 90 pp 143-153

[Article by S.D. Borovkov, S.A. Grishenkov, V.P. Novikov, Ye.V. Serga, A.V. Kharlamov, and Yu.S Khodyrev]

[Abstract] Use of optical transition radiation for diagnostic testing of 70 GeV proton beams extracted from the U-70 accelerator (quickly within less than 5 μs and slowly within less than 1 s) and in apparatus for their nondestructive testing was studied experimentally. The theory of this method is based on the characteristics of optical transition radiation emitted by a relativistic charged particle, normally or obliquely entering a material from an ambient vacuum and then reentering a vacuum. Theoretical relations have been derived for the quantity $d^2N_\lambda/d\Omega d\lambda$ which, upon integration, will yield the number of photons of wavelength λ emitted into a unity solid angle Ω: emitted forward by protons entering vacuum and emitted backward by protons entering the material, the total number of photons in each direction being the sum of those with the polarization axis parallel to the proton beam and of those with the polarization axis perpendicular to it. Conditions of the experiment are accounted for by considering the number of photons emitted by a proton beam with some space distribution within the plane of transition radiation emission and recorded with a special purpose LI450 television camera, a vidicon with a CdSe target, in a plane normal to the direction of that emission at some distance from the proton source. The experiment was performed with two aluminum targets, one 35 nm thick on a mylar substrate and one 500 nm thick on a polyimide substrate. Optical transition radiation was measured with a digital television camera on a movable platform. The targets were inserted into the proton beam by a mechanism so as to make protons impinge on the aluminum coating on the polymide film normally and on the aluminum coating on the mylar film at a 45° angle. The threshold sensitivity of this camera for 680 nm radiation, at the wavelength of maximum sensitivity, was $2.4.10^{-7}$J/m^2 or 8.10^5photons/mm^2, the quantum efficiency of its target being 0.67 and its spectrum covering 0.61 of the optical transition radiation spectrum. Measurements were made according to a special program, the beam image being first encoded by an 8-digit analog-to-digital converter for processing by a computer and subsequent graphic display. The algorithm of measurements and data processing took account of background conditions, the principal source of noise being particles impinging on the glass screen and faceplate of the vidicon. These measurements have yielded the angular distribution of photons. The results are in sufficiently close agreement with theoretical formulas for optical transition radiation emitted by highly relativistic protons at angles much smaller than $\min(\psi, \pi/2 - \psi, |\varepsilon - 1|)$, measurement error being readily eliminated in the course of data processing. Measurement of integral luminous fluxes was found to be much more immune to background noise when done with digital television apparatus than when done with photomultipliers. The conditions for nondestructive inspection of proton beams from an accelerator on the basis of optical transition radiation should, moreover, be more favorable than they were in the experiment, owing to its higher luminous output and its more narrow angular distribution. Figures 7; tables 1; references 14.

UDC 538.22

Topology and Magnetic Solitons in Collinear Antiferromagnetics

907J0031C Kharkov FIZIKA NIZKIKH TEMPERATUR in Russian Vol 16 No 2, Feb 90 pp 242-246

[Article by I.A. Leonov, Institute of Single Crystals, Kharkov, and V.L. Sobolev, Donetsk Institute of Engineering Physics, UkSSR Academy of Sciences]

[Abstract] Existence of topological solitons other than homotopic nontrivial ones in a perfect crystal of an antiferromagnetic material is examined, considering that topological solitons covering large distances in anisotropic media form a "domain wall with edge" or a line of intersection of several domain walls. In an antiferromagnetic material of the NiO type with a T-wall between radial domains; for instance, collinearity of spins inside the wall is not maintained on account of topological factors. Description of the wall between any possible domains in a perfect crystal requires inclusion of four antiferromagnetism vectors l_i (i = 1,2,3,4) corresponding to sublattices $r_{i_1}+r$ and three unit vectors i,j,k along fourth-order axes, magnetostrictive distortion of a crystal being disregarded. An analysis based on this premise indicates that only non-topological, two-dimensional magnetic solitons can exist in a perfect crystal of an antiferromagnetic material, but that interaction of magnetic solitons and flaws in a defective crystal can be described in topological terms. References 8.

Dependence of Emission of Light Charged Particles With Up to 400 MeV/Nucleon Energy on Mass of Bombarding Nucleus

907J0040A Moscow YADERNAYA FIZIKA in Russian Vol 51 No 4, Apr 90 pp 936-941

[Article by V.A. Antonchik, S.D. Bogdanov, A.Yu. Likharev, and V.I. Ostroumov, Leningrad Polytechnic Institute, V.Ye. Dudkin and N.A. Nefedov, Institute of Biomedical Problems, USSR Ministry of Public Health]

[Abstract] Another experiment in the photoemulsion series was performed concerning fragments of a target nucleus, including charged particles with less than 400 MeV/nucleon energy after collision of the target nucleus with an incident one. Nuclei of photoemulsion with a C,N,O light

component and a Br,Ag heavy component were bombarded in 242 events by ^{40}Ar carrying an energy of 1.2 GeV/nucleon. All secondary particles have been subdivided into two energy classes: singly-charged protons into slow ones with less than 30 MeV/nucleon and fast ones with 30-400 MeV/nucleon, doubly-charged alpha particles into slow ones with less than 10 MeV/nucleon and fast ones with 10-400 MeV/nucleon. The data obtained in this experiment on both kinds of particles include their average multiplicities , average angles of exit , average energy average transverse momentum, and average longitudinal momentum. The data are compared with results of calculations on the basis of the cascaded-evaporation model covering 4091 numerical simulation events and are added to earlier experimental data covering bombardment of heavy, as well as light, photoemulsion nuclei by nuclei ranging from ^{22}Ne to ^{56}Fe so as to establish how those characteristics of secondary protons and alpha particles in each energy class depend on the mass of the incident nucleus. This dependence is described by a linear approximating binomial = $a_0+a_1A_t$ (A_t-mass of incident nucleus) for each characteristic y of secondary particles on the basis of chi-square statistics, and found to affect fast particles much more than slow ones. Noteworthy are the different values of a_1 indicating that light or heavy target nuclei emit protons with a larger longitudinal momentum, but at a smaller angle than alpha particles, and the different values of a_0 that heavy target nuclei emit any kind of second particle at a larger angle, but with a lower energy as well as a lower longitudinal momentum than do light target nuclei. The most likely and simple explanation for these differences is that relatively more interaction involving substructures of incident nucleus and protons of the target nucleus take place when the mass of the incident nucleus is larger. Figures 4; tables 3; references 13.

Fission of ^{233,236,238}U and ^{239}Pu Nuclei in (d,pf) or (t,pf) Reactions With Slow Incident Particles

907J0040B Moscow YADERNAYA FIZIKA in Russian Vol 51 No 4, Apr 90 pp 942-951

[Article by M.F. Andreyev, Yu.M. Bolshakov, V.V. Gladkov, V.A. Zavgorodniy, and V.I. Serov]

[Abstract] An experimental study was made concerning fission of U and Pu nuclei in low-energy reactions ^{233}U(d,pf) with E_d = 11 MeV, ^{233}U(t,pf) with E_t = 12.7 MeV, ^{236,238}U(t,pf) with E_t = 12.56 MeV, and ^{239}Pu(d,pf) with E_d = 11.7 MeV. Fission fragments were picked up by four semiconductor-type detectors at 65°, 155°, -45°, and -140° angles to the incident particle (deuteron, triton) beam respectively. Protons were recorded, with an energy resolution of approximately 100 keV, by two ΔE-E telescopes of such detectors at 120° and -70° angles to the incident deuteron beam respectively. The data have been processed by the method of least squares and then approximated with the first even Legendre polynomial P_2, adequate for an evaluation of both energy and angular distributions of the fission fragments. The results indicate a changing yield of neutrons and γ-quanta in these reactions at certain levels of excitation energy, the most likely cause of this being a redistribution of fission fragments with respect to mass or kinetic energy at those excitation levels. Figures 8; tables 1; references 15.

Scattering Matrix for Stochastic Systems With Many Degrees of Freedom

907J0040C Moscow YADERNAYA FIZIKA in Russian VOL 51 No 4, Apr 90 pp 1001-1007

[Article by S.N. Yezhov, Kiev State University, and V.A. Plyuyko, Institute of Nuclear Research, UkSSR Academy of Sciences, Kiev]

[Abstract] In an application of statistics to nuclear reactions, calculation of the mean scattering matrix for a stochastic system by a method simpler than the perturbation method is extended to a system of statistically nonequivalent reaction channels. With the Hamiltonian of such a system expressed in the form $H = H_0+V$ (H_0-mean field, V-random residual interaction), a symmetric and unitary scattering matrix for such a system with given parity and total spin is written in the form $S = USU^{-1}$ (where $S = I-iR$, $R = F^TQF$, $Q = (E-H_0-V+iFF/2)^{-1}$, (U-NxN unitary matrix, V,F-real random matrices of ΛxΛ and ΛxN dimensionalities respectively). Following an orthogonal O-transformation which diagonalizes the symmetric real matrix $E-H_0-V$ matrix and then yields the trace $Sp\ Q = G_\lambda(E)$, integral equations are obtained for the average Green functions of the non-self-adjoint Hamiltonian $H_0+V-iFF^T/2$ and g(z) of the energy operator H_0+V. These equations describe the dependence of the elements of a Gaussian scattering matrix on the binding force as well as on the force of residual interaction between discrete-spectrum states and continuous-spectrum states. They are solved analytically and then numerically for the case where the H_0 Hamiltonian has an equidistant discrete spectrum of finite width ΔE with a density of levels $\rho_0(E) = 1/D$ in the $|E| = or < \Delta E/2$ band and $\rho_0(E) = 0$ in the $|E| > \Delta E/2$ band. The authors thank V.M. Strutinskiy for helpful discussion. Figures 4; references 27.

Effect of T-Odd Electron Nucleon Interaction on Propagation of Light Through a Medium

907J0040D Moscow YADERNAYA FIZIKA in Russian Vol 51 No 4, Apr 90 pp 1056-1062

[Article by M.G. Kozlov and S.G. Porsev, Leningrad Institute of Nuclear Physics, USSR Academy of Sciences]

[Abstract] Manifestations of direct T-odd electron-nucleon interaction in a medium are analyzed theoretically, one such manifestation being its effect on the propagation of light through that medium. Interaction of

light and medium in a constant electric field is considered, inclusion of T-odd interaction in the atomic Hamiltonian, leading to a dependence of the refractive index on the longitudinal component of the electric field. First, an expression is derived for the potential of T-odd but P-even electron-nucleon interaction, only one combination of such an interaction being possible. Next are calculated the phase shift along the light propagation path and then, by the diagram method, the T-odd interaction in thallium as a typical heavy element. The authors thank A.N. Moskalev for participation and interesting comments, and V.P. Gudkov for helpful discussions. Figures 3; references 11.

Production of Neutrino-Antineutrino Pairs From Neutrino in Field of Strong Electromagnetic Wave

907J0040E Moscow YADERNAYA FIZIKA in Russian Vol 51 No 4, Apr 90 pp 1076-1080

[Article by R.V. Konoplich, Moscow Institute of Engineering Physics]

[Abstract] Production of neutrino-antineutrino pairs during interaction of the magnetic moment of a neutrino and the field of a plane electromagnetic wave in a heavy-particle accelerator is analyzed theoretically. Taken into consideration, is the wave function of a neutral fermion, with some magnetic moment, satisfies the generalized Dirac equation. Calculations are based on the corresponding effective Lagrangian in the static limit and on the probability of such a process in terms of producing a unit volume in a unit time. The results indicate that such a process cannot yet be detected experimentally at the present state of the art, unless there exist neutral fermions with an anomalously large magnetic moment. The author thanks Yu.P. Nikitin. References

UDC 537.58:546.31

Thermal Stability of Compressed Hydrogen Atom at 10,000-20,000 K Temperatures: Calculation by Monte Carlo Method

907J0043D Moscow TEPLOFIZIKA VYSOKIKH TEMPERATUR in Russian Vol 28 No 1, Jan-Feb 90 pp 1-9

[Article by S.V. Shevkunov, Leningrad Institute of Electrical Communications Engineering]

[Abstract] The quantum-mechanical version of the Monte Carlo method, based on Feynman integrals over trajectories, is applied to a hydrogen atom inside a spherical cavity with a radius L = 0.2 nm at 10,000-20,000 K temperatures, for a calculation of the radial electron density distribution. The trajectory of an electron is represented by M = 160 vertices and so, as to remove the nonphysical singularity of the Coulomb potential on the nucleus due to finite-dimensional approximation of limiting Feynman trajectories, the r^{-1} vertex-nucleus interaction potential is replaced with a $u(r) = e^2 \log [(\delta^2 + (2r)^2)^{1/2} + \delta / [(\delta^2 + (2r)^2)^{1/2} - \delta$ potential characterizing interaction of a "point" nucleus and a uniformly charged segment $\delta = (\beta/M)^{1/2}$ of an electron trajectory. A comparison of this electron density distribution with one calculated analytically on the basis of the ground state indicates that, besides the estimated 3-4 percent statistical error of the Monte Carlo method, there are no systematic errors in the use of limiting Feynman trajectories. The wave function and the ground-state energy of a hydrogen atom inside a spherical cavity are, for reference, calculated on the basis of the Schroedinger equation and its series solution with an appropriate recurrence relation for the series coefficients. Figures 2; references 17.

UDC 538.221

Solitons in Modulated Magnetic Structure of MnOOH and Isomorphic Compounds

907J0048A Leningrad FIZIKA TVERDOGO TELA in Russian Vol 32 No 1, Jan 90 pp 212-219

[Article by A.B. Borisov and V.V. Kiselev, Institute of Metal Physics, Ural Department, USSR Academy of Sciences, Sverdlovsk]

[Abstract] The spectrum of spin waves propagating above modulated magnetic structures is analyzed, such structures forming in monoclinic crystals of antiferromagnetic compounds such as MnOOH and isomorphic with it $Mn_{1-x}A_xOOH$ where A denotes a nonmagnetic ion. From the Landau-Lifshits equation for two magnetic vectors, in either ferromagnetic or antiferromagnetic domains of such a structure, is derived a simpler equation for one vector which correctly describes nonlinear free energy and magnetization dynamics in this system in the quasi-one-dimensional localized excitation approximation. This equation reduces even simpler, exactly integrable Boussinesq equation in the case of weak nonlinearity, when only acoustic modes are generated. Application of the reductive perturbation theory transforms this equation into the Korteveg-deVries equation and thus leads to the existence of a soliton solution, which implies a "transparence" of modulated magnetic structures to nonlinear spin waves. References 13.

UDC 621.78:661.66:549.212

Effect of Carbon Recrystallization in High-Pressure Chamber on Structure of Synthesized Diamond Polycrystals

907J0051A Moscow DOKLADY AKADEMII NAUK SSSR in Russian Vol 311 No 3, Mar 90 pp 613-616

[Article by V.P. Polyakov, V.P. Yelyutin, corresponding member of USSR Academy of Sciences, N.I. Polushin, S.A. Perfilov, and V.V. Lapin , Moscow Institute of Steel and Alloys]

[Abstract] An experimental study concerning synthesis of diamond polycrystals in a high-pressure chamber was made, its object being structural changes in the carbon material during the heat treatment and their effect on the diamond structure. Tests were performed in two chambers, a lenticular one and a toroidal one, using in each, first, only soot produced by pyrolysis of methane and than a mixture of such soot with 20 wt.% 63/40 Ni-Mn alloy powder. The original soot consisted of small imperfect crystals. Raising the temperature was found to induce ordering and recrystallization of this material. Under high pressure, it was found to recrystallize into higher-density graphite, this process being accelerated by shearing stresses built up under nonhydrostatic pressure. Metallographic and x-ray examination of specimens produced under pressures of 3.3-7.7 GPa at temperatures of 1750-2070 K has revealed the pressure and temperature dependence of the soot graphitization process and of the graphite structure prior to graphite → diamond transformation. When such a transformation did not take place, graphite was found to have become impregnated with Ni-Cr alloy melt. Inasmuch as the capillary pressure in graphite pores, of the order of 20 μ in diameter, is estimated to be not higher than 0.2 GPa, metallization of graphite is evidently caused by the usual high pressure drop built up in the chamber for synthesis of diamond polycrystals. Figures 1; table 2; references 7.

UDC 539.172

Delayed Fission of Excited Heavy Nuclei

907J0053B Moscow DOKLADY AKADEMII NAUK SSSR in Russian Vol 310 No 6, Feb 90 pp 1357-1360

[Article by Yu.V. Melikov, S.Yu. Platonov, A.F. Tulonov, O.V. Fotina, and O.A. Yuminov, Scientific Research Institute of Nuclear Physics at Moscow State University imeni M.V. Lomonosov]

[Abstract] A theoretical explanation is given for the experimentally discovered new phenomenon, namely a time delay of stimulated fission of heavy nuclei. Based on an analysis of relevant experimental data and calculations pertaining to nuclei of elements in the actinide series such as ^{232,233}Pa and ^{235,236,237,238,239}Np, a correlation is found between the delay time and the depth of the second potential well. Fission of these nuclei evidently proceeds much slower than their decay along any other reaction channel, this delay being in some way related to the lifetime of excited states in the second potential well. This is confirmed by the dependence of the mean decay time, the density of excited states on the excitation energy and by the dependence of the decay delay time on the difference B_f^{min}-ΔE (B_f^{min}-height of lowest barrier to fission, ΔE-energy difference between ground states in first well and in second well). Article was presented by Academician G.N. Flerov. Figures 3; references 10.

UDC 539.194.01

Effect of Interference of Lines on Form of Infrared Bands Perturbed by Coriolis Interaction

907J0066A Leningrad OPTIKA I SPEKTROSKOPIYA in Russian Vol 68 No 3, Mar 90 pp 539-544

[Article by M.V. Kudryashov and N.N. Fillippov]

[Abstract] The form of infrared bands appearing in absorption spectra as a result of vibrational-rotational interactions and perturbed by Coriolis interactions is analyzed theoretically, starting from the corresponding Hamiltonian of a spectroscopically active molecule $H = H_{rot} + H_{vib} + H_{VR}$ (H_{VR}-Coriolis interaction operator). Two vibrational bands are considered within the frequency range of transitions from vibrational ground state to states of A_1 and A_2 kinds, these states being components of an anharmonic l-split of a strongly excited vibrational state of a molecule with C_{3v}- symmetry (l-quantum number of projection of vibrational angular momentum on C_3-axis of such a molecule). Dipole transitions from the vibrational ground state to the A_2-sublevel being forbidden, the two absorption bands within this range are evidently associated with "mixing" of the two components by Coriolis interaction and resulting emergence of two new mixed states. Dependence of the two rotational constants on the vibrational state is disregarded and the model of strong collisions is used, for simplicity. Calculations are made in the fixed laboratory system of coordinates, the orientation of a molecule in this system being described by three Euler angles. These calculations, the dependence of both the contour form characterized by the spectral function $F(\omega)$ and of the normalized band half-width on the normalized speed of rotational relaxation. The spectral function is the real part divided by π of an integral transform from 0 to infinity of the correlation function $C(t)$ characterizing the dipole moment of a molecule, the expression for that correlation function becoming simple in the Markov approximation and in the formalism of a spectral lines space. This calculated contour of the $\nu_4+\nu_5$ (A_1,A_2) band of a CF_3Cl molecule in Ar at 90 K temperature agrees roughly with the one estimated on the basis of experimental data. The authors thank D.N. Shepkin, T.D. Kolomiytsev, S.M. Melikov, and V.A. Kondaurov for discussion and helpful comments. Figures 2; references 15.

Energy Losses Incurred by Neutrino in Matter

907J0069A Moscow ZHURNAL EKSPERIMENTALNOY I TEORETICHESKOY FIZIKI in Russian Vol 97 No 4, Apr 90 pp 1089-1102

[Article by D.A. Kirzhnits, V.V. Losyakov, and V.A. Chechin, Institute of Physics imeni P.N. Lebedev, USSR Academy of Sciences]

[Abstract] The energy loss incurred by a neutrino passing through matter is evaluated theoretically in the "collision" limit. Taken into consideration, is the energy loss

is extremely small on account of the weak neutrino-matter interaction and the question is posed about whether there exist media in which collective effects could appreciably increase that loss. On the basis of fundamental relations, including the Hamiltonian of a particle and the density matrix of a "particle + medium" system, a theory is constructed which first yields the energy losses incurred by a charged Dirac particle and then those incurred by a neutrino, the neutrino-medium interaction Hamiltonian having a 4-fermion form and five characteristics of the medium ($R_{1,2}^{a}$, d_{v}, R_{A} or $d_{1,2}^{a}$) being needed for analysis of the problem rather than only two in the case of a charged particle. The collision limit is then considered, nonrelativistic matter being regarded as a degenerate slightly nonideal electron gas on a positively charged substrate. Its response function is calculated accordingly, the Leontovich dispersion relation is shown to apply here. A universal upper bound for the neutrino energy loss is established on this basis, namely the collision limit for a muon neutrino independent of its energy and 0.6-2.8 times the collision limit for an electron neutrino depending on its energy. No medium at equilibrium anomalously slowing down a neutrino is shown to exist. The authors thank participants of the seminar chaired by V.L. Ginzburg, A.A. Komar, and A.Ye. Chudakov, as well as L.B. Leinson, V.N. Orayevskiy, V.B. Semikoz, Ya.A. Smorodinskiy, and V.N. Ursov for discussions. Figures 2; references 14.

Microwave Photoconductivity of Mesoscopic System

907J0069E Moscow ZHURNAL EKSPERIMENTALNOY I TEORETICHESKOY FIZIKI in Russian Vol 97 No 4, Apr 90 pp 1317-1320

[Article by A.A. Bykov, G.M. Gusev, and Z.D. Kvon, Institute of Semiconductor Physics, Siberian Department, USSR Academy of Sciences]

[Abstract] An experimental study of a mesoscopic system, a strip of GaAs film consisting of δ-doped layers with a random potential, and consequently an asymmetry between electrons above and holes below the Fermi level, has confirmed the theoretically predicted anomalous behavior of its photoconductivity with a nonmonotonic frequency dependence under the influence of microwave electromagnetic radiation. Long specimens of such strips were 0.5-1 μm wide and, after they had been plasmochemically etched, potentiometer probes were placed on them 2-3 μ apart with the driving-point voltage between them not exceeding kT/e. The photoconductivity was measured at 1.4-4.2 K temperatures in a magnetic field of up to 3 T by the current-voltage method, with an active 7 kHz a.c. bridge, while the specimens were exposed to microwave radiation amplitude modulated by a 120 Hz signal. The specimens were treated with 6-8 GHz radiation fed through a cable directly to the current terminals and with 30-80 GHz radiation fed through a waveguide terminating into a polarizer. The dependence of the photoconductivity on the intensity of the external magnetic field at various microwave frequencies was found to be characterized by aperiodic oscillations of the photoconductivity about a positive constant level. These oscillations became sufficiently wide to reduce the photoconductivity to zero or make it negative at some levels of the magnetic field intensity. The pattern of these oscillations was also found to depend on the frequency of the microwave radiation, the frequency dependence of photoconductivity being different from the field dependence of the conductance within the 6-8 GHz "low" frequency range and being similar to the latter within the 30-89 GHz "high" frequency range. Also, the field dependence of the conductance in the absence of microwave radiation was measured for reference and for extraction of the magnetoconductance component. On the basis of the data, the correlation functions of photoconductivity fluctuations and photogalvanic effect fluctuations have been calculated, an analysis of the results indicating that a strong high-frequency electric field completely suppresses mesoscopic fluctuations of the magnetoconductance and thus a close correlation of photoconductivity oscillations magnetoconductance oscillations. However, this close correlation could also be attributed to heating of the electron gas. The pattern of aperiodic photoconductivity oscillations within the low-frequency range indicate a nonthermal contribution to photoconductivity of a mesoscopic system. The authors thank V.I. Falko for divulging the results of his study prior to their publication, D.I. Lubyshev and V.P. Migali for supplying the specimens, and M.R. Baklanov for performing the plasmochemical treatment. Figures 2; references 8.

New Data on Phase Transitions of CsI and Its Equation of State (Role of Hydrostaticity)

907J0069F Moscow ZHURNAL EKSPERIMENTALNOY I TEORETICHESKOY FIZIKI in Russian Vol 97 No 4, Apr 90 pp 1321-1325

[Article by I.V. Aleksandrov, A.F. Goncharov, I.M. Makarenko, and S.M. Stishov, Institute of Crystallography imeni A.V. Shubnikov, USSR Academy of Sciences]

[Abstract] An experimental study of CsI single microcrystals was made involving their isothermal compression under pressures up to 52 GPa at room temperature in a diamond anvil with helium as the hydrostatic pressure transmitting medium, and a subsequent phase analysis in a DRON-2.0 x-ray diffractometer. The pressure dependence of the density of CsI crystals and of the interplanar distances in them indicates that hydrostatic compression does not, as had been surmised earlier, transform the CsI crystal lattice into a closest-packed-cubic one. A comparison of the results with those of previous studies made by other authors indicates that a nonhydrostatic pressure distribution in the compressing medium can introduce large errors into pressure readings and needs to be corrected; only the "hydrostatic" compression curve agrees with the theoretical curve based on the equation of state and calculations by the method of attached waves. Figures 4; references 17.

UDC 539.4.019.3:539.1.04

Photodestruction of Mechanically Stressed Nylon-6

907J0097a Leningrad FIZIKA TVERDOGO TELA in Russian Vol 32 No 5, May 90 pp 1350-1355

[Article by T. B. Boboyev, Kh. D. Dadomatov, T. F. Abdunazarova, M. P. Vershinina, N. G. Kvachadze, E. Ye. Tomashevskiy, Engineering Physics Institute imeni A. F. Ioffe at the USSR Academy of Sciences, Leningrad]

[Abstract] The effect of tensile stress on photodestruction of nylon-6 [kapron] is examined by irradiating an oriented polymer with ultraviolet light at wavelengths of 254, 313, and 365 nm. Oriented monofibers (fishing lines), films, and filaments were used as samples. Destruction kinetics were analyzed by the development of free radicals and the decrease in the molecular mass. The radical concentration was measured by the EPR method and the molecular mass, by the viscometry method. The results confirm that the stressed polymer state affects the photodestruction kinetics by increasing the radical yield and the number of ruptures and make it possible to establish the correlation between the radical accumulation, bond breaking, and strength degradation on the one hand and the stressed sample accumulation on the other. It is also found that the number of ruptures in irradiated films increases almost linearly over time within a given stress range. The photodestruction rate rises with the applied stress and with a decrease in the excited light wavelength. The ratio of the number of broken bonds to the number of light quanta absorbed is determined and the dependence of the quantum yield of the bond breaking on tensile stress is established for various wavelengths. The dependence of the strength degradation on stress was established in the 20-140°C temperature range at $\lambda = 254$ nm. The results also show that longwave nylon-6 thread irradiation leads to a smaller strength degradation than shortwave irradiation in both stressed and nonstressed samples. References 17: 15 Russian, 2 Western; figures 6.

UDC 539.89:539.213

Transition of High-Pressure GaSb Crystalline Phase to Amorphous State

907J0097b Leningrad FIZIKA TVERDOGO TELA in Russian Vol 32 No 5, May 90 pp 1429-1432

[Article by V. F. Degtyareva, I. T. Belash, Ye. G. Ponyatovskiy, V. I. Rashchupkin, Solid State Physics Institute at the USSR Academy of Sciences, Chernogolovka, Moscow Oblast]

[Abstract] Amorphization conditions of Ga-Sb binary alloys are examined radiographically. The results show that gallium antimonide and similar Ga-As alloys spontaneously pass to an amorphous state from a quenched crystalline high-pressure β-Sn phase obtained by high-pressure heat treatment at 90 kbar and 150-300°C. The correlation between the alloys' amorphization ability, T_c temperature of the β-Sn phase, and high-pressure treatment temperature, as well as the presence of a certain β-Sn phase homogeneity, make it possible to speculate that the amorphization process is related to the loss of atomic ordering which is characteristic of the initial stoichiometric GaSb compound. References 13: 6 Russian, 7 Western; figures 1.

UDC 537.312.62

Effect of Layered Structure on Vibratory Spectra in Bismuth and Thallium High-T_c Superconductors

907J0097d Leningrad FIZIKA TVERDOGO TELA in Russian Vol 32 No 5, May 90 pp 1565-1568

[Article by I. P. Ipatova, Yu. E. Kitayev, V. G. Malyshkin, R. A. Evarestov, Engineering Physics Institute imeni A. F. Ioffe at the USSR Academy of Sciences, Leningrad]

[Abstract] $(Tl/Bi)_2(Ba/Sr)_2Ca_{n-1}Cu_nO_{2n+2}$ compounds with an *I4/mmm* spatial symmetry are examined. Optical spectra of such crystals were identified by a theoretical group analysis of phonons in high-T_c superconductor (VTSP) crystals, whereby a bulk crystal is examined as a three-dimensional periodic system. *LIII* layers were analyzed. The analysis shows that in these layers some two-phonon layer states, which are inactive in second order processes, generate bulk states which are active in second order Raman scattering and second order infrared absorption in the *z*-polarization but the corresponding spectral line strength is rather low. References 12: 7 Russian, 5 Western; figures 1; tables 1.

Origin of Gamma-Radiation Observed From Crab and Vela Pulsars at 1 TeV Photon Energy

907J0101a Moscow PISMA V ZHURNAL EKSPERIMENTALNOY I TEORETICHESKOY FIZIKI in Russian Vol 52 No 10, 10 Jul 90 pp 655-658

[Article by S. V. Bogovalov, Yu. D. Kotov, Moscow Engineering Physics Institute]

[Abstract] A statistically significant photon flux at energies over 10^{11} has been observed from just a few sources, including two radio pulsars: Crab and Vela. Photons at such energies in pulsars with a magnetic field of close to 10^{12} G must be produced far from the neutron star. Only in this case, the γ-quantum conversion to an $e'e$ pair would not prevent the escape of radiation from the source. For the fast-spinning Crab and Vela pulsars, the free γ-quanta escape region starts near the light cylinder area. Superhard γ-radiation spectra are analyzed. It is shown that this radiation forms near the light cylinder during the Compton backscattering of relativistic electrons on the neutron star's thermal radiation photons. A

correlation of γ-ray bursts and those in soft X-rays with an energy of about 1 keV is predicted. References 13: 5 Russian, 7 Western; figures 1.

Electron Accommodation and Stimulated Emission of Electrons During an Interaction of a Beam of Vibrationally Excited Hydrogen Molecules With the Surface of α-Al_2O_3

907J0106g Moscow ZHURNAL EKSPERIMENTALNOY I TEORETICHESKOY FIZIKI in Russian Vol 98 No 1(7), Jul 90 pp. 226-238

[Article by V. P. Grankin, N. A. Savinkov, V. V. Styrov, Yu. I. Tyurin, Mariupol Metallurgical Institute]

[Abstract] Energy transfer from the vibrationally excited molecules to electrons in a crystal was observed directly for the first time with the help of the electron accommodation method developed by the authors. Excited molecules reach the surface directly from the gaseous phase in the form of an H_2 molecular beam rather than being produced on the surface as in earlier experiments. The surface of aluminum oxide in a metastable state was excited beforehand by ultraviolet light. The resulting "supplementary" electron excitation of trap electrons at the expense of vibrational energy led to an electron emission. Vibrational energy transfer from the excited gaseous phase molecule to localized electron states in a dielectric crystal virtually refutes earlier notions and demonstrates that the electron system participates equally in relaxation processes in the gas-solid system. The transfer occurs by means of an electron-dipole (quadrupole) interaction between the electrons and the variable dipole (quadrupole) moment of the vibrating molecule. At higher vibrational energies attained by laser pumping or in an exothermic reaction, energy is also transferred to electrons due to the nonadiabatic vibratory-electron coupling. References 22: 17 Russian, 5 Western; figures 4.

Efficiency of Polarized Phase Conjugation in Optical Fiber-Crystal System

907J0008A Leningrad PISMA V ZHURNAL TEKHNICHESKOY FIZIKI in Russian Vol 16 No 4, 26 Feb 90 pp 4-8

[Article by A.V. Volyar, N.V. Kukhtarev, L.M. Kuchikyan, S.N. Lapayeva, and V.V. Muravyev, Simferopol State University imeni M.V. Frunze]

[Abstract] Recovery of polarization during phase conjugation in a system consisting of an optical fiber and a photorefractive crystal is considered, phase conjugation by such a crystal not being equally efficient for incident light beams linearly polarized in different directions. The problem is analyzed and calculations are made for unperturbed and perturbed fibers transmitting only a few modes which do not interact. Linearly polarized laser radiation passes through such a fiber, then through a polarization prism which splits it into two orthogonally polarized beams. Both pass through a crystal in which they undergo phase conjugation and then return through the same fiber where they recover the original polarization. The scheme was studied experimentally with a He-Ne laser as light source and a $Bi_{12}TiO_{20}$ crystal for phase conjugation. A converging microobjective lens was inserted between the prism and the fiber entrance, a collimating one was placed behind the fiber exit. Between that lens and the phase conjugating crystal were inserted a semitransparent plane mirror at a 45° angle and a polarizer with the axis orthogonal to the direction of light polarization. The mirror split the incident light beam into two: one being transmitted for normal passage through the polarizer and the crystal in the x-direction, one being deflected to a fully reflecting plane mirror for lateral passage through the crystal without polarizer in the y-direction. Another fully reflecting plane mirror behind the crystal returned the second beam through the crystal to the first reflecting mirror, back to the beam-splitter and to the optical fiber. The complex reflection coefficients of the crystal were $R_x = 0.11$ and $R_y = 0.06$ for 630 nm light. Theoretical analysis is based on transformation of the Maxwell vector-columns representing the split of a linearly polarized mode by dispersion in the fiber into two natural modes with different propagation constants. Calculations for this system yield 0.91-0.99 maximum and 0.66-0.74 minimum efficiency of phase conjugation with recovery of only one polarization, namely the one collinear with that of the original incident light beam. The author thanks the staff members at the Institute of Engineering Physics, USSR Academy of Sciences, who have supplied the photorefractive crystal. Figures 2; references 10.

UDC 535.8

Radiation Emission by H + Xe Mixtures Near Craft Models Flying at High Supersonic Speeds

907J0054A Moscow TEPLOFIZIKA VYSOKIKH TEMPERATUR in Russian Vol 28 No 2, Mar-Apr 90 pp 338-344

[Article by O.V. Zverev and N.N. Pilyugin, Institute of Mechanics, Moscow State University imeni M.V. Lomonosov]

[Abstract] A gas mixture of hydrogen and xenon has been selected for numerical simulation and analysis of radiation emission by mixtures of hydrogen and an inert gas near models of craft flying at high supersonic speeds, after mixtures of hydrogen and helium had been studied experimentally in aeroballistic model tests. The equilibrium composition of a H + Xe mixture as well as its temperature and pressure behind a forward compression shock near the stagnation point under conditions simulating aeroballistic tests with velocities within the N_{Ma} = 30-40 range of the Mach number are calculated on the basis of the Rankin-Hugoniot relations, considering that the gas mixture consists of two components not chemically reacting with each other and taking into account ionization of each. Both the emissivity and the absorptivity of such a mixture are then calculated, considering that recombination emission of ions and bremsstrahlung of electrons in ion and atom fields are the two principal processes which govern the continuous radiation emission by inert gases. For hydrogen in the continuous spectrum, transitions considered were free-free transitions in the H-atom and [illegible] ion field, also six free-free transitions with six diff[illegible] photoionization thresholds. For hydrogen in the discrete spectrum, the lines considered were the three most intense lines of the Lyman series ($L_{\alpha,\beta,\gamma}$) and the two most intense lines of the Balmer series ($H_{\alpha,\beta}$). With the aid of these data is then analyzed radiative heat transfer in H + Xe mixture according to the Stefan-Boltzmann law. Figures 5; references 12.

UDC 537.635

New Kind of Magnetic Resonance in Cubic Strongly Anisotropic Ferromagnet

907J0057A Leningrad FIZIKA TVERDOGO TELA in Russian Vol 33 No 3, Mar 90 pp 762-764

[Article by A.S. Lagutin and A.V. Dzhitriyev, Institute of Atomic Energy imeni I.V. Kurchatov, Moscow]

[Abstract] Inversion of levels in the Tb^{3+} ion in mixed ferrimagnetic $Y_{3-x}Tb_xFe_5O_{12}$ garnets by action of an external magnetic field has been demonstrated experimentally by magnetic resonance measurements. Two such garnets with a low Tb content were tested at 4,2 K temperature, cubic single crystals with x = 0.1 and x = 0.26 respectively, in pulsed magnetic fields of up to 40 T intensity, parallel to the [110] plane. Measurements were made with millimetric electromagnetic radiation from backward-wave traveling tubes over the 35-96 GHz frequency range, a helium-cooled InSb crystal serving as detector. These measurements have yielded the field of the magnetic resonance frequency, this resonance frequency being proportional to the field intensity within the weak-field range below 5 T. Absorption of microwave radiation by these crystals in strong fields correlates closely with observed anomalies in the field dependence of their differential magnetic susceptibility. Resonance in magnetic fields of about 3.5 T intensity

($Y_{2.9}Tb_{0.1}Fe_5O_{12}$) or 7-8 T intensity ($Y_{2.74}Tb_{0.26}Fe_5O_{12}$) and in magnetic fields of higher than 20 T intensity (both garnets) can thus be associated with inversion of original levels in the Tb^{3+} ion and with reversal of magnetism in the rare-earth subsystem respectively. Figures 4; references 5.

Thin-Film High-Frequency SQUID's With Microbridge Junctions

907J0060A Leningrad ZHURNAL TEKHNICHESKOY FIZIKI in Russian Vol 60 No 3, Mar 90 pp 135-140

[Article by I.Yu. Antonova, V.M. Zakosarenko, Ye.V. Ilichev, V.I. Rozenflants, and V.A. Tulin, Institute of Problems in Technology of Microelectronics and Extra-Pure Materials, USSR Academy of Sciences, Chernogolovka (Moscow Oblast)]

[Abstract] Three kinds of microbridge junctions were studied for use in radio-frequency SQUID's. The material selected for superconducting thin films was niobium, on account of its high mechanical strength combined with high chemical stability and adequate superconductivity characteristics. KDB-10 silicon was selected as substrate material, plates of this material being commonly used in microelectronics and having a sufficiently high electrical conductivity at room temperature. Films were deposited on substrates by sputtering an Nb target in a high-frequency magnetron with a power density of 4.1 W/cm^2, the residual gas pressure prior to deposition not exceeding 50 μPa and the working argon pressure during deposition amounting to 0.1 Pa. Impurities had been removed from the substrates by etching in a high-frequency discharge. Entrapment of gaseous impurities during growth of films at a rate of 2-2.5 nm/s, without special heating or cooling of the substrates, was prevented by application of a negative voltage, 40-60 V, to the substrates in the process. Microbridges of variable thickness were deposited through a mask with a 0.8-2.0 μm wide working gap. This method yielded microbridges at a rate of 70 per cycle on substrate disks 76 mm in diameter, but with a wide spread of parameters so that only 2 percent of them had a critical current below 100 μA and a hysteresis-free current-voltage characteristic. Anodization of microbridges in an aqueous solution of $NaNO_3$ under a stabilized voltage would lower any high critical current within the 100-500 μA range to less than 100 μA, without inhibiting superconductivity along the banks. This process yielded microbridges with a critical current I_c = 50 μA and I_cR_N = 1 mV. Microbridges of submicron dimensions were produced by electron-beam lithography. In this process 0.3-0.4 μm thick Nb resist films were deposited, dried at 170°C for 30 min (ERP-40 resist) or at 189°C for 40 min (ERP-9 resist) prior to exposure to a dose of 10 C/μm charge in an automatic electron-beam lithographer with a ZRM-12 microscope, and then developed in 1:3 mixture of metaloethyl ketone + isopropyl alcohol at 22°C temperature for 30 s (ERP-40 resist) or 15 s (ERP-9 resist). The residual resist layer was used as mask for protection of the films during their subsequent plasmochemical etching in a SF_6 + O_2 gas stream. This process yielded microbridges with a 10 percent fraction in the I_c = 20-100 μA and I_cR_N = 0.3-0.5 mV class. Microbridges of the SNS sandwich kind were produced by standard microelectronic technology, beginning with photolithographical deposition of an FP-383 photoresist mask, a periodic grating of 3 mm wide strips with a 6 mm pitch, on the Si substrate for subsequent plasmochemical etching of the latter through to the necessary 0.1-0.3 μm depth. The mask was then removed so that a two-step stair remained on the substrate. A film of copper or gold was deposited on this stair by vapor condensation from a tungsten crucible under vacuum, with the substrate oriented so as to make the copper or gold stream impinge on its surface at an angle smaller than 5° but normally to the edges. In this way the deposited Cu or Au film grew to 70 nm thickness on the riser and to less than 5 nm thickness on the two steps. The substrates, thus coated with films of normal metal, were placed in a magnetron for deposition of niobium, after a preliminary cleaning operation with an argon plasma and removal of all excess normal metal above the 5 nm thickness. The thickness of the Nb film was smaller than 0.2 μ on the steps and approximately 50 nm on the riser. With a positive electron resist covering the Nb film, the latter was by electron-beam lithography and then plasmochemical etching split into two level steps connected by a riser. This process yielded microbridges with I_cR_N = 0.3-0.5 mV. All three versions of microbridge junctions were installed in a hybrid high-frequency (30 MHz) test SQUID and, after their performance had been found to be satisfactory, in an experimental thin-film SQUID for a feasibility study. The results indicate that such a thin-film SQUID has a lower current/flux sensitivity than the best SQUID's with point junctions, but is more reliable and stable owing to its mechanical robustness. Figures 6; references 7.

UDC 535.215.9

New Prospects in Electrooptics

907J0063 Leningrad OPTIKA I SPEKTROSKOPIYA in Russian Vol 68 No 4, Apr 90 pp 723-726

[Article by N.A. Tolstoy and A.A. Spartakov]

[Abstract] Extensive studies concerning the luminescence and electrooptical properties of colloidal solutions have established that any colloid particle or other suspension particle smaller than 10 μm in a polar dispersion medium has a giant dipole movement proportional to the surface area of such a particle, independent of the substance but dependent on the substance of the dispersion medium. These characteristics of the giant dipole is attributable to spontaneous unilateral orientation of the molecules of a polar dispersion fluid and resulting formation of an electric "domain" adjacent to those dipoles. The attendant electrooptic effects may be accompanied by electrooptical effects associated with anisotropy of the electrical polarizability, these two kinds of electrooptic effects being readily segregated by

methods of rotating electric fields. Three such fields are described here, each transverse to the light beam passing through the cell with colloidal dispersion. An r_1-field, with a constant magnitude E-vector, rotates some constant speed usually within the 0.1-20 Hz range influencing both the dipole movement and the polarizability anisotropy of colloidal particles. The latter rotate following the field at some angle behind it and thus modulate the polarized light; the dipole movement often, but not always, dominating the polarizability anisotropy. An r_2-field is one whose E-vector not only rotates at some constant speed but also oscillates through a 180° angle at a frequency much higher than that speed. Here, there is not enough time for rigid dipole orientation reversal of colloid particles and the latter rotate behind the field only by virtue of polarizability anisotropy. An r_3-field is one whose E-vector also rotates at some constant speed and oscillates, but only through a 90° angle, at a frequency much higher than that speed. The rotating field acts only on the dipole movement of colloid particles, striving to orient them along the bisector of the angle which determines the amplitude of oscillations, while the torque produced by action of the rotating field on the polarizability anisotropy only reverses its sign at that frequency. An analysis of the last two methods, based on the equation of motion of a particle in the respective rotating field, indicates that the r_3-field method is applicable not only to rotating-field electrooptics, but also to "linear" electrooptics and to molecular liquids as well as to colloidal systems. Existence of a giant dipole movement is most effectively demonstrated and the relative contributions of this dipole movement and polarizability anisotropy are most correctly evaluated by combination of both r_2-field and r_3-field methods. The authors acknowledge the contribution by Petr Petrovich Feofilov to this research conducted at the State Institute of Optics imeni S.I. Vavilov. Figures 1; references 7.

UDC 530.182.551.510.42

Possible Traces of Laser Radiation From Earth's Atmosphere

907J0064A Tomsk OPTIKA ATMOSFERY in Russian Vol 3 No 4, Apr 90 pp 390-393

[Article by G.S. Bordonskiy, Chita Institute of Natural Resources, Siberian Department, USSR Academy of Sciences]

[Abstract] Traces of laser action on earthly objects and particularly on window glass have been occasionally observed, as for instance in Chita on 16 April 1984 at about 4 PM, when a hole 6 cm in diameter was found in the outer window pane on the third floor of a building facing northwest. Research and analysis of data have led to the hypothesis that laser radiation originates in the upper layer of Earth's atmosphere and arrives on Earth in narrow pulsed beams. Validation of this hypothesis will require further measurements of incoming radiation within the atmosphere's infrared, ultraviolet, and microwave transparence windows. This is especially true during magnetic storms and while the Earth is crossing the boundaries between sectors of the interplanetary magnetic field, within regions where bolides have burst and within regions of geomagnetic and radiation anomalies. Figures 2; references 8.

UDC 522.617:535.3.087

Potential Resolution of Images Formed by Passive Methods Through Turbulent Atmosphere, Part 1: Speckle Interferometry in Conventional Telescopes

907J0064B Tomsk OPTIKA ATMOSFERY in Russian Vol 3 No 4, Apr 90 pp 394-397

[Article by P.A. Bakut, I.A. Rozhkov, and A.D. Ryakhin]

[Abstract] Image formation through a turbulent atmosphere by methods of speckle interferometry is analyzed for highest attainable resolution, based on a statistical model of image distortion by such an atmosphere. The simplest case is considered viewing a stationary object through a conventional telescope and formation of its images by a series of M short exposures. The resolving power of speckle interferometry is characterized by the ratio Q of the dispersion of brightness fluctuations to the dispersion of the error of brightness estimates made on the basis of those short exposures. This ratio is calculated with recording noise taken into account, but only randomness of the photon count and resulting irremovable quantum effects being considered. This ratio increases monotonically, to some maximum, as the spectral band is widened and the recording time lengthened. The accuracy of this ratio depends on the width of the object, when the latter is smaller than or equal to the average resolving power of the atmosphere, becoming maximum when the width of the object is about equal to the diffractional resolving power of the telescope; it is independent of the width of the object when the latter is much larger than the resolving power of the atmosphere. The accuracy of this ratio Q depends on the Fried radius or space correlation radius of atmospheric distortions and is directly proportional to the number M of recorded images. The highest attainable resolving power is almost independent of the telescope's diffractional resolving power, when it is not smaller than the latter. Numerical estimates based on theoretical and experimental data pertaining to Mercury, Venus, and the Moon yield a highest attainable image resolution $1/2.10^7 M^{1/4}$rad(2.10^{-8} with $M = 10^4$ and a D = 25 m aperture diameter). References 14.

UDC 522.617:535.3.087

Potential Resolution of Images Formed by Passive Methods Through Turbulent Atmosphere , Part 2: Speckle Interferometry in Synthesized Telescopes

907J0064C Tomsk OPTIKA ATMOSFERY in Russian Vol 3 No 4, Apr 90 pp 398-403

[Article by P.A. Bakut, I.A. Rozhkov, and A.D. Ryakhin]

[Abstract] Speckle interferometry in nonredundant multiaperture-synthesized reflecting telescopes, such as the VLT with a 104 m base and others with low occupancy of subapertures, is analyzed for the possibility of attaining image resolutions of the order of 10^{-8} rad or higher on the basis of M short exposures. The analysis is based on description of short-exposure images by their space-frequency spectrum, mathematically equivalent to the brightness distribution and obtained from the latter by a Fourier transformation. The optical transfer function of an isoplanatic atmosphere-telescope system is calculated first, the accuracy of this transformation depending on the ratio Q of the actual space spectrum of the object image squared to the mean error of its estimate squared. Subsequent calculation of that ratio for an object of small angular width, with an effective correlation radius of its space spectrum larger than the effective correlation radius of atmospheric distortions in the composite telescope aperture, yields, on the basis of realistic numerical values, a highest attainable resolution $1/10^{-6}M^{1/3}$rad (10^{-7} with $M = 10^3$ exposures, 2.10^{-8} with $M = 10^5$ exposures) and thus better than the highest attainable one in a conventional telescope. Figures 2; references 15.

Phase Conjugation During Second-Harmonic Generation in Oligomodal Fibers

907J0068A Moscow PISMA V ZHURNAL EKSPERIMENTALNOY I TEORETICHESKOY FIZIKI in Russian Vol 51 No 8, 25 Apr 90 pp 389-392

[Article by B.Ya. Zeldovich and Yu.Ye. Kapitskiy, Chelyabinsk Polytechnic Institute]

[Abstract] An experiment has demonstrated the possibility of phase conjugation on gratings with square-law polarizability in optical fibers sustaining several transverse modes at both second-harmonic frequency and fundamental frequencies. The experiment was performed with a Nd laser emitting 100 ps radiation pulses in packets of 30 at a repetition rate of 4000 Hz. During passage through a KTP crystal a part of this radiation was converted into second-harmonic, whereupon a prism split the mixture of both into two parallel beams. A microobjective coaxial with fiber focused both beams on the fiber entrance to make the infrared fundamental-frequency beam enter the fiber axially and the visible second-harmonic beam enter the fiber at some angle to its axis, following off-center passage through the lens. Radiation leaving the fiber was focused by an identical second microobjective on a photodiode for power measurement, which yielded approximately 0.2 W of infrared radiation and 0.005 W of visible radiation. For recording chi-square holograms, radiation leaving the KTP crystal was passed through a prism and a filter which cut off the second-harmonic component. It was then reflected by set mirrors for entering the fiber at the other end, after passage through a plane-parallel plate and the second microobjective. Passage of radiation through the fiber in opposite directions was found to produce second-harmonic radiation, recorded on a KN-4 photographic film after passage through that first microobjective and reflection by a sliding mirror. Gratings were first recorded, for rough estimates, with a 4° lead-in angle between the fundamental-frequency beam and the second-harmonic beam. Subsequent recording with the lead-in angle varied over the 0-8° range by rotating the plane-parallel plate, revealing a bilinear dependence of the lead-out and recording angle of the second-harmonic beam on the lead-in angle between the two beams, with a 1:1 slope from 0° to 4° and a 1:4 slope from 4° to 8°. The readout indicated that phase conjugation of the second-harmonic waves had taken place, inasmuch as neither the attitude nor the form of the second-harmonic distribution, but only its intensity level, varied during rotation of the plane-parallel plate. The authors thank N.B. Baranov, R.H. Stolen, and V.M. Churikov for helpful discussions. Figures 3; references 6.

UDC 621.373.2

Correcting Thermal Distortions of Light Propagating Through Medium With Phase Conjugating Stimulated-Brillouin-Mandelshtam-Scattering Mirror

907J0072A Tomsk OPTIKA ATMOSFERY in Russian Vol 3 No 2, Feb 90 pp 174-181

[Article by O.I. Vasilyev and S.S. Lebedev, Scientific-Industrial Association 'Tayfun', Obninsk]

[Abstract] The feasibility of using phase conjugation by an SBMS (stimulated Brillouin-Mandelshtam scattering) mirror for compensating thermal distortions of a periodically pulsed laser beam, propagating through the atmosphere of the Earth, is examined on the basis of a mathematical model and a laboratory experiment. The duration of the laser pulses is assumed to be sufficiently short and the interval between, sufficiently long, for no self-induced thermal distortions to take place so that the only thermal distortions will be those caused by heating of the medium by preceding laser pulses. The mathematical model for numerical simulation consists of a wave equation for the complex amplitude of the electric field E in a medium with a temperature-dependent dielectric permittivity and an equation describing the dynamics of the temperature field $T(x,y,z,N\Delta t)$ (Δt-time interval between successive laser pulses, N-number of laser pulses). In the experiment, a beam of 489 nm light, 5 mm in diameter, from a continuous-wave Ar-laser was passed through a splitter plate with a 0.20 reflection coefficient into an absorption cell containing ethyl alcohol with

fuchsin dye, this medium with a 0.04 cm^{-1} absorption coefficient simulating the atmosphere of Earth. The beam power was varied over the 0-0.8 W range. The cell, 30 cm along the beam, was moved across the latter back and forth at a velocity of 0.33 cm/s. Absorption of the laser radiation by the medium and consequent heating of the latter induced a nonuniform distribution of the refractive index. The absorption cell was probed with a Nd-laser beam of 530 nm second-harmonic radiation in pulses of 0.3 J energy and 40 ns duration above the half-amplitude level, this beam countering the Ar-laser beam not quite collinearly at a 1.5 mrad angle. While passing through the cell, this probing laser beam became distorted by the nonuniform refractive index distribution which the Ar-laser beam had induced by heating. Following passage of the probing beam through the absorption cell, the probing beam was focused by lens into another cell containing CCl_4 for stimulated Brillouin-Mandelshtam scattering with attendant reflection by such a mirror. Power and angle measurements at each stage, with and without the SBMS mirror, have yielded data on the radiation distribution in the probing laser beam. These experimental data, together with theoretical calculations including a compensation accuracy analysis based on the geometrical parameters of the system, indicate that it may be possible to compensate thermal distortions of a periodically pulsed laser beam in a stirred medium by means of a phase conjugating SBMS mirror. The authors thank B.S. Agrovskiy and A.S. Gurvich for valuable suggestions. Figures 5; references 8.

UDC 621.373.826

Potential Characteristics of Phase Conjugation Algorithm for Observation of Large Objects

907J0072B Tomsk OPTIKA ATMOSFERY in Russian Vol 3 No 2, Feb 90 pp 182-187

[Article by V.Ye. Kirakosyants, V.A. Loginov, and V.V. Slonov, Scientific-Industrial Association 'Astrofizika', Moscow]

[Abstract] The performance of a phase conjugation algorithm for observation of large objects with diffusely reflecting surfaces is analyzed for efficiency of signal energy utilization. The performance indicator is selected, the ratio of the transmission coefficient, when the object is a real one, to the transmission coefficient when the object, ideally, would be a reflecting one in a homogeneous ambient medium and the receiver, noiseless. The multichannel receiver part includes a heterodyne oscillator which also serves as master oscillator in the transmitter part, the latter includes a multichannel amplitude-and-phase modulator and a laser amplifier. Two modes of radiation transmission to the object are considered, with the signal energy spread over the entire object or focused on a given point of the object as the limiting case. The general relations obtained for each mode are applied to an adaptive observation apparatus with phase conjugation operating in the iterative probing mode. The maximum attainable efficiency of such an apparatus is calculated for various values of the system parameters. This includes those which characterize the size of the object, assuming a large number of channels and a high signal-to-noise ratio, but taking into account strong distortion of the signal wavefront by strong multiplicative interference generated by roughness of the object surface. The number of iterations necessary for attaining that maximum efficiency and thus ensuring the expected advantage over a nonadaptive observation apparatus is determined as a function of the object size. Stabilization is approached as the number of channels approaches infinity and the length of time to reach it increases with the size of the object. Tables 3; references 5.

Optoacoustic Multifrequency Light Wave-Front Pickups

907J0099a Leningrad PISMA V ZHURNAL TEKHNICHESKOY FIZIKI in Russian Vol 16 No 8, 26 Apr 90 pp 9-12

[Article by L. V. Balakin, V. I. Balakshiy, Ye. V. Tsukerman]

[Abstract] Wave front pickups are used in laser physics, adaptive optics, nondestructive control systems, etc. A wave front pickup, in which the sound carrier frequency varies from train to train by a discrete value within a given frequency band, is examined. Compared to high spatial resolution wave front pickups and real time pickups, based on optoacoustic scanners; the multifrequency optoacoustic pickup examined in this experiment makes it possible to analyze the phase structure of the light field with a random amplitude distribution in the light wave front. It has a broader measurement range of the light wave incidence angles upon the optoacoustic cell, and can be easily linked to a computer to process data on the light wave phase structure. The authors are grateful to F. A. Chudnovskiy for discussing the results. References 3; figures 2.

Optical Properties of Shock-Compressed Inert Gas Plasma. Wide-Range Model Comparison to Experiments

907J0099c Leningrad PISMA V ZHURNAL TEKHNICHESKOY FIZIKI in Russian Vol 16 No 8, 26 Apr 90 pp 74-77

[Article by A. Ya. Polishchuk, V. Ye. Fortov, High-Temperature Institute at the USSR Academy of Sciences, Moscow]

[Abstract] To judge the credibility of the wide-range model describing Coulomb collisions, its results must be compared to experimental data for plasma of typical nonmetallic inert gases at 10^{19}-$10^{22}cm^{-3}$ densities and temperatures of several eV. It is shown that, despite its approximate nature, the wide-range model adequately describes fine optical phenomena of plasma bleaching

related to a delocalization of excited electron states of atoms. To analyze this phenomenon, the mathematical description of the electron state delocalization was modified. The specific values of the parameters were established by comparing them to experimental data. The quantitative applicability of equations, describing the plasma bleaching effect, was considered. Experimental results are consistent with an analysis in the framework of a bounded atom model, making it clear that the photoionization contribution is suppressed, with an increase in density, and absorptance asymptotically approaches the bremsstrahlung limit. Thus, the wide-range model adequately describes not only the metal to dielectric transition in the near-critical area and the successive ionization due to the pressure of internal electron shells, but also the fine effects related to the highly excited atomic state delocalization. References 15: 8 Russian, 7 Western; figures 1.

Multilayer Normal Incidence Mirrors for Extreme Ultraviolet Radiation

907J0100a Leningrad ZHURNAL TEKHNICHESKOY FIZIKI in Russian Vol 60 No 5, May 90 pp 85-96

[Article by A. A. Vasilyev, S. V. Gaponov, S. A. Gusev, V. V. Dubrov, I. G. Zabrodin, A. I. Kuzmichev, B. M. Luskin, N. N. Salashenko, V. A. Slemzin, I. I. Sobelman, A. P. Shevelko, Applied Physics Institute at the USSR Academy of Sciences, Gorkiy]

[Abstract] The results of studies of the plane and spherical multilayer mirror characteristics in the 125-450 angstrom wavelength and experiments to focus X-rays and obtain an image using spherical mirrors are described. The main experiments were conducted with Mo-Si based mirrors, whereby multilayer structures were applied by electron beam evaporation in a vacuum chamber with a pressure limit of about 10^{-9} torr. The layer thickness was monitored and the deposition process was controlled automatically with the help of a crystal thickness gauge and a quadrupole mass spectrometer. Special attention was given to reducing the multilayer structure interplane roughness related to the deposition method, and the mirror substrate roughness. The mirrors had a peak reflectance of about 20 percent. The experiments reveal that such mirrors may be used to obtain an image with a close to 1 μm resolution in the ultrasoft X-radiation. The possibility of shaping intense directional radiation from high-temperature plasma is demonstrated. A radiant intensity of 10^7W/cm^2 in the λ = 182 angstrom band was obtained in the laser plasma image plane. References 32: 5 Russian, 27 Western; figures 7; tables 2.

UDC 533.951

Charged Particle Acceleration by Strong Langmuir Waves in Nonuniform Plasma Flows

907J0102a Moscow FIZIKA PLAZMY in Russian Vol 16 No 7, Jul 90 pp 795-800

[Article by S. V. Bulanov, V. V. Gavrishchaka, General Physics Institute at the USSR Academy of Sciences]

[Abstract] One of the principal advantages of accelerating particles by plasma waves is the possibility of attaining high longitudinal electric field intensities and phase velocities necessary for synchronism with the accelerated particles. A mechanism which makes it possible to enhance the excited plasma wave, thus controlling its phase characteristics, is considered. It is suggested that plasma with a monotonically varying density, in which current is induced by external sources, be used. An analysis of the method shows that in nonuniform plasma with a steady-state current configuration, one can improve amplitude and phase characteristics of the Langmuir wave in nonuniform plasma in order to accelerate the particles during the wave passage through the area of inhomogeneity. Both one- and two-dimensional cases were examined. For the two-dimensional geometry, the possibility of both amplifying the wave amplitude and adjusting the phase velocity to an optimal value is demonstrated. In the one-dimensional case, it is possible to effectively amplify relativistic and weakly relativistic Langmuir waves, thus increasing the acceleration tempo. Numerical estimates are cited. The authors are grateful to A. G. Shkvarunts for useful discussions. References 9: 6 Russian, 3 Western; figures 3.

UDC 533.951

Nonlinear Langmuir Wave Amplification in Plasma With Regular and Random Magnetic Fields

907J0102b Moscow FIZIKA PLAZMY in Russian Vol 16 No 7, Jul 90 pp 801-805

[Article by V. S. Krivitskiy, Yu. M. Pryadko, V. N. Tsytovich, General Physics Institute at the USSR Academy of Sciences]

[Abstract] Studies of the prospect for amplifying high-frequency waves due to their nonlinear interaction with some low-frequency plasma oscillation modes, in resonance (Cherenkov or cyclotron) with plasma particles, are drawing considerable attention. A rather common case of the presence of both random and regular magnetic fields, either in laboratory (e.g., tokamak) or cosmic plasma is examined; two types of perturbation, low- and high-frequency, are considered. It is established that when Langmuir oscillations propagate in plasma with regular and random magnetic fields, the "plasma maser" effect may occur; whereby its magnitude is proportionate to the square of the external magnetic field and inversely proportionate to the fifth power of the Langmuir wave frequency. The dependence of the wave attenuation decrement on the angle between field vectors in an isotropic medium is derived. The energy up-conversion enhancement by the resonance oscillation spectrum anisotrpy is established. The greatest Langmuir wave energy up-conversion with frequency occurs in the case of an anisotropic plasma particle distribution function. The wave amplification increment in this case may be on the order of the plasma frequency. References 15: 5 Russian, 10 Western.

UDC 517.958

New General Solution Representations of Stokes' System of Equations

907J0103a Moscow DOKLADY AKADEMII NAUK SSSR in Russian Vol 312 No 1, May 90 pp 76-80

[Article by N. V. Saltanov, Fluid Mechanics Institute at the Ukrainian Academy of Sciences, Kiev]

[Abstract] The problem of obtaining different representations of the general solution of Stokes' equations calls for additional studies, both from the viewpoint of expanding mathematical approaches to its solution and its applications. The results of an investigation into this problem on the basis of a specially introduced generalized potential for the so-called nonuniform part of the solution, which is similar to the generalized potential in the theory of gas dynamic flows suggested earlier by the author, are presented. It is shown that this approach makes it possible to derive a general solution of Stokes' system of equations with the help of the method of separation of variables in the same frames of reference, as in the case of Helmholtz vector equation. A transition to known representations of Lamb, Happel and Brenner is made in spherical and circular coordinates, respectively. Finally, a representation is cited which is an analogue of the Papkovich-Neuber representation of the solution of Lame's equation widely used in the theory of elasticity. The results of this study may be useful in analyzing slow viscous fluid flows on the basis of Stokes' equations. The article is submitted by Academician Yu. A. Mitropolskiy. References 11.

Model of Self-Induced Fluctuation Superconductivity

907J0055A Moscow PISMA V ZHURNAL EKSPERIMENTALNOY I TEORETICHESKOY FIZIKI in Russian Vol 51 No 9, 10 May 90 pp 465-467

[Article by V.G. Karpov and D.A. Parshin, Leningrad Polytechnic Institute imeni M.I. Kalinin]

[Abstract] A new model is proposed to describe the emergence of superconductivity following a phase transition of the first kind (gas-to-liquid kind) superconductor materials with an easily changeable structure, i.e., in materials containing mobile structural defects such as impurities or vacancies. The model, which covers every mechanism of superconducting condensation and conceptually resembles the flux ion model, is based on the dependence of the local superconducting transition temperature T_c on the local defect concentration c. This dependence being, in the simplest case, a linear one; the fluctuation temperature term added to the average critical temperature is equal to the deviation of local from average defect concentration δc multiplied by a tentatively positive constant. According to this model, moreover, at temperatures below T_c superconducting condensation of electrons or displacement of mobile defects decreases the free energy by $\delta F_1 = V\alpha^2(T_c-T)^2/2b$. (V-volume of fluctuation region, α,b-Ginzburg-Landau parameters). Meanwhile, fluctuations increase the free energy by $\delta F_2 = -T\delta S$ (δS-change of entropy). This increment is in the quadratic approximation, assumed to be proportional to $(\delta c)(\delta c+c_{aver})/c_{aver}\delta c$. On the basis of this model is established and calculated the dependence of the net change of free energy δF_1-δF_2 on the deviation from average defect concentration. The rate at which S-phase regions of entropy fluctuations form depends on the height of the thermodynamic barrier to phase transition and on the defect diffusion coefficient. This is demonstrated by two examples: freeze-in of high-temperature thermodynamic defect concentration fluctuations during fast cooling and nucleation of critical S-phase regions at low temperatures. The authors thank Yu.M. Galperin, V.I. Kozub, and E.B. Sonin for helpful discussion. Figures 2; references 9.

UDC 539.21:537.1:548:537.1

Superconductivity of Dipole-Polaron System

907J0057B Leningrad FIZIKA TVERDOGO TELA in Russian Vol 32 No 3, Mar 90, pp 867-870

[Article by V.A. Kovarskiy, Institute of Applied Physics, MSSR Academy of Sciences, Kishinev]

[Abstract] Existence and properties of a dipole-polaron system in lanthanum ceramics are examined, these ceramics theoretically having a metal-like electrical conductivity, but behaving like dielectrics in experiments. This paradox is resolved by considering that the apparently half-occupied v_2' band near the symmetric center points Γ, X really consists of an empty band v_2'' and an occupied band v_2. Analysis of the problem is based on calculating the energy of holes, relative to the Fermi-level, and the energy of hole-hole interaction in a polar medium with a refractive index n, a static relative dielectric permittivity ε_0, and an optical phonon frequency ω. An expression for the corresponding interaction potential W(r) is obtained with the aid of the Riemann-Mellin transformation. The results are applied to tetragonal La_2CuO_4 ceramic with $n^2 = 5$, $\varepsilon_0 =$ or > 15, $\omega = 500$ cm^{-1}, Froehlich constant $\alpha_F = 5$, and $|m_2|$ approximately equal to 0.5 m_1, in which case the Riemann zeta function does not come close to unity. The collective properties of a hole gas according to this model of hole-hole interaction calculated from the Hamiltonian in the Fermi operators formulation, with the aid of the Bogolyubov uv-transformation, and by the variational method. In this way, the chemical potentials of a dipole-polaron gas in its bound states are obtained, particularly important being its lowest excited 1s-state corresponding to a pair of free holes. The chemical potential of a rare dipole-polaron gas is found to remain finite, even as the gas concentration approaches zero, and to become negative as the gas concentration reaches 10^{16}cm^{-3}. An energy gap of a finite width, 90 cm$_{-1}$ at this concentration, will then appear, like in an ideal Bose-gas, but not in a dense Fermi-gas or dense exciton gas with hardly any bound states. The width of the energy gap, therefore, depends nonmonotonically on the dipole-polaron concentration. Applicability of the Bose-concentrate model of superconductivity to a dipole-polaron gas is validated on the basis of the band structure and the effective mass. Figures 1; references 15.

UDC 537.312:538.945

Improving Mechanical Properties of Ta-Y-Ba-Cu-O Superconducting Metal Oxide

907J0061A Kiev DOKLADY AKADEMII NAUK UKRAINSKOY SSR, SERIYA A: FIZIKO-MATEMATICHESKIYE I TEKHNICHESKIYE NAUKI in Russian No 4, Apr 90 pp 59-62

[Article by V.N. Varyukhin, A.T. Kozakov, S.N. Loboda, and B.A. Panasyuk, Institute of Metal Physics, UkSSR Academy of Sciences, Kiev]

[Abstract] An experimental study of the superconducting metal-oxide system $YBa_2Cu_3O_{7-d} + \gamma Ta_2O_5$ with various magnitudes of the γ fraction was made for a determination of its electrical and mechanical properties depending on the phase composition. Specimens of these materials were produced by adding $\gamma = 0.01$-0.3 Ta_2O_5 to the 1:2:3 mixture of Y_2O_3 + BaO + CuO for synthesis at 970-980°C temperature by a 12 h long process. The product was cooled down and then pulverized, whereupon the powder was compacted into 8 mm long plates 2x8 mm^2 in cross-section under a hydrostatic pressure of 12-15 kbar. These were sintered at the same 970-980°C

temperature for another 12 h, but in an oxygen atmosphere. Specimens with $\gamma = 0.01, 0.03, 0.05, 0.1, 0.2, 0.3$ were tested for superconductivity based on the temperature dependence of their electrical resistivity and magnetic susceptibility, their critical temperature found to be 92-90 K within a 1-2 K wide transition range. Their phase composition was determined under a scanning electron microscope with a Camebax-Micro x-ray spectrum microanalyzer and, statistically, on polished fragments, also with an 09 IOS-3 Auger-electron spectrometer on fresh microsections. All materials were found to have a polyphase composition; three phases having been identified in addition to the Y-Ba-Cu-O 123-phase: Y_2BaCuO_5, CuO, and $Ta_{0.5}Y_{0.5}Ba_2CuO_5$. The hardness of specimens was measured by the standard method on the basis of 30-50 indentations. The results indicate that the mechanical properties of Y-Ba-Cu-O materials can be improved by doping them with Ta atoms preferably along the grain boundaries, without degradation of their superconducting transition at 92-90 K temperature. Evidently, their mechanical properties are also improved by structural transformation of one component phase induced by internal stresses. Synthesis of a pure $Ta_{0.5}Y_{0.5}Ba_2CuO_5$-phase material should be regarded as a further step in that direction. Article was presented by Academician V.G. Baryakhtar, UkSSR Academy of Sciences. Figures 2; tables 1; references 8.

UDC 291.19.29.22.16.06

Dependence of Critical Current for $YBa_2Cu_3O_{7-d}$ Superconductor Ceramic on Size of Specimen

907J0062A Minsk IZVESTIYA AKADEMII NAUK BSSR: SERIYA FIZIKO- MATEMATICHESKIKH NAUK in Russian No 2, Mar-Apr 90 pp 45-47

[Article by T.Ye. Zhabko, F.P. Korshunov, L.F. Makarenko, N.M. Olekhnovich, O.I. Pashkovskiy, V.K. Shesholko, and V.D. Yanovich, Institute of Solid-State and Semiconductor Physics, BSSR Academy of Sciences]

[Abstract] An experimental study of $YBa_2Cu_3O_{7-d}$ high-temperature superconductor ceramic was made, for the purpose of determining how the critical current depends on the geometrical dimensions of a specimen. Specimens of this material were produced by standard technology from a mixture of Y_2O_3, $BaCO_3$, CuO powders, with synthesis and sintering at temperatures of 850-950°C, followed by annealing in an oxygen stream. Electrical measurements were made on two lots of specimens, low-density ones (H-17, H-80) and high-density ones (141/88, 146/88) with respectively 70-79 percent and 90 percent of the x-ray diffraction limit. The oxygen deficiency did not exceed $d = 0.1$ in all specimens. Electrical measurements were made by the current-voltage method through silver contact tabs; the critical current had been determined as the transport current which produced a voltage drop not larger than 0.1 mV. The cross-section of specimens was decreased in two different ways so as to neutralize any possible effect structural diversity and material nonhomogeneity have on the readings. It was decreased either by cutting a specimen into approximately two halves along the current path, and then necking down each "half" specimen in the middle between the potential contact tabs or by stepwise slicing off equally thick layers on both sides, parallel to and symmetrically, with respect to the axis along the current path and thus always leaving a center core. The critical current density was found to become higher with decreasing cross-section, no matter how the latter had been decreased. The field dependence of the critical current density was, for all specimens, found to follow the relation $J_c = J_{c0}/[1+(H_a/H^*)^m]$ ($m = 1.8$-2.2, H^*-intensity of external magnetic field at which the critical current density is equal to half the critical current density J_{c0} in absence of an external magnetic field H_a). On the basis of the experimental data and calculations, according to the VanDuser-Turner model, for sufficiently thick specimens that zero-field critical current density should be proportional to one-third power of the cross-section area S. Figures 2; references 5.

UDC 539.373:548.03:535.36

Electronic Excitations and Radiative Defects in Metal-Oxide Dielectrics

907J0065B Riga IZVESTIYA AKADEMII NAUK LATVIYSKOY SSR: SERIYA FIZICHESKIKH I TEKHNICHESKIKH NAUK in Russian No 2, Mar-Apr 90 pp 29-37

[Article by Ch.B. Lushchik, F.A. Savikhin, E.H. Feldbach, I.V. Bitov, H.R. Joegi, and I.A. Kudravtseva, Institute of Physics, ESSR]

[Abstract] Defects developing in high-temperature metal-oxide superconductor materials of Y-Ba-Cu-O and Bi-Ca-Sr-Cu-O classes are examined on the basis of available theoretical and experimental research data, including experimental data obtained by the authors. The overview covers post-irradiation suprathreshold effects produced by bombardment with high-energy particles, as well as subthreshold effects, attending decay of electronic states as possible mechanisms of defect formation at 300 K temperature with the material in the normal state, and at 10 K temperature with the material in the superconducting state; these effects had been revealed in the spectra of cathodoluminescence, ultrashort luminescence, and diffuse reflection. Great importance is finally attached to stabilization of the superconducting collective in those materials against recombination with excess current carriers. An experimental study of intraband-transition luminescence and its temperature dependence had revealed that this may be possible when equilibrium current combine into the superconducting collective. The authors thank A. Maaroos, and I Meriloo for synthesizing the crystals of

metal-oxide ceramics, P. Liblik, T. Leyb, and V. Korsakov for assisting in the experiments. Figures 4; references 24.

Stimulation of Superconductivity by Impurities

907J0068B Moscow PISMA V ZHURNAL EKSPERIMENTALNOY I TEORETICHESKOY FIZIKI in Russian Vol 51 No 8, 25 Apr 90 pp 399-402

[Article by V.P. Mineyev, Institute of Theoretical Physics imeni L.D. Landau, USSR Academy of Sciences]

[Abstract] Nonmagnetic impurities in low concentrations do not influence the temperature at which transition into a superconducting state with s-pairing occurs, but do suppress all other modes of superconductivity so that the respective critical temperatures drop proportionally to the concentration of such an impurity when the latter scatters electrons elastically, while magnetic impurities suppress superconductivity with s-pairing as well. Inelastic scattering of conduction electrons by two-level impurity centers is analyzed by taking into account the attendant change in the energy of these electrons and transition of the impurity into excited states. The analysis is based on Eliashberg and Abrikosov-Gorkov methods. When applied to the heavy-fermion $U_{1-x}Th_xBe_{13}$ series, it yields a nonmonotonic Th-concentration dependence of the critical temperature, above the critical temperature T_{c1} for intrinsic UBe_{13} with the critical temperature peaking to T_m when the Th concentration reaches some level x = m and, then again, dropping as the Th concentration is further increased. It seems that only when U atoms are being replaced by Th atoms can a transition from coherent scattering when $x < x_m$ or $T < T_m$ to noncoherent including inelastic one when $x > x_m$ or $T > T_m$ occur prior to complete suppression of superconductivity with T_c still above zero. When at some threshold Th concentration T_c drops to zero while T_m remains above zero, which happens under pressure, then T_c can be raised again and superconductivity restored only by some still higher Th concentrations at which T_m will be zero. The author thanks G.Ye. Volovik, G.M. Eliashberg, A.M. Dyugayev, A.M. Finkelshteyn, and V.G. Marikhin for discussion. Figures 1; references 6.

Change in Superconductor and Electrical Characteristics of $Bi_2Sr_2CaCuO_x$ Material Under High Pressure

907J0068C Moscow PISMA V ZHURNAL EKSPERIMENTALNOY I TEORETICHESKOY FIZIKI in Russian Vol 51 No 8, 25 Apr 90 pp 411-414

[Article by Ye.A. Alekseyeva, I.V. Berman, N.B. Brandt, A.A. Zhukov, I.L. Pomashkina, and V.I. Sidorov, Moscow State University imeni M.V. Lomonosov]

[Abstract] An experimental study of $Ba_2Sr_2CaCuO_x$ single crystals was made, the object being changes in the temperature dependence of their electrical resistance over the 1.5-300 K temperature range, as the pressure was raised to 160 kbars. The specimens were 300 mm long, 30 mm square bars with thin low-resistance silver-paste contact tabs fused on by heat treatment in an oxygen stream with special temperature-time cycling, for resistance measurement by a simulation of the four-point method. Pressure was produced on a Bridgman anvil. On the basis of the data, curves had been plotted depicting the temperature dependence of the resistance, with the linear superconducting transition range extrapolated to a fictitious, somewhat lower temperature of transition onset and to a somewhat higher zero-resistance temperature of transition end, also curves depicting the reversible pressure dependence of these two temperatures, as well as, the temperature corresponding to the middle of the transition range. These curves indicate that single crystals of this material retain their superconductivity under pressure up to 158 kbars. The nonlinear descent of both upper and middle transition temperatures over a rather wide spread and the attendant increase of the dT_c/dP derivative with rising pressure are not typical of most high-T_c metal-oxide superconductors or most classical superconductors, and the pressure-induced changes in the temperature dependence of their electrical resistance were rather analogous to changes which characterize amorphous semiconductors as the metal-to-dielectric transition is approached. Figures 3; references 11.

Galvanomagnetic Properties and Fermi Surface of Organic Superconductor β-$(ET)_2IBr_2$ Material

907J0069C Moscow ZHURNAL EKSPERIMENTALNOY I TEORETICHESKOY FIZIKI in Russian Vol 97 No 4, Apr 90 pp 1305-1315

[Article by M.V. Kartsovnik, P.A. Kononovich, and I.F. Shchegolev, Institute of Solid-State Physics, V.N. Laukhin and S.I. Pesotskiy, Institute of Chemical Physics, USSR Academy of Sciences]

[Abstract] An experimental study on organic superconductors in the (ethylenedithio)tetrathiofulvalene group, namely β-$(ET)_2IBr_2$ was made for a thorough investigation of its galvanomagnetic properties in strong magnetic fields. Perfect single crystals of this material were tested for magnetoresistance characteristics, namely its angular distribution over the -90-(+90)° sector and field dependence over the 80-150 kOe range at 1.5-4.2 K temperatures. The electrical resistance of these crystals was less than 2000 times lower at 4.2 K than at 300 K. It was measured along the a-axis and along the c-axis crossing the high-conductance ab-plane, with an 11.7 Hz alternating current of 1 mA through thin Au contact tabs and Pt electrodes designed for measurement of low-temperature resistances within the 10-30 mohm range with a relative error smaller than 5.10^{-4}. The magnetic field was produced by a superconducting solenoid, inside which specimens could be rotated in the three ab, ac*, b'c* planes (c* perpendicular to ab, b' perpendicular to ac*). The results reveal Shubnikov-deHaas oscillations: "slow" ones at a frequency about 0.5 MG noticeable in a

magnetic field perpendicular to the b'-axis while at an angle within -25-(+5)° to the c*-axis sector and "fast" ones at a frequency of about 40 MG noticeable within a much wider range of angles with the c*-axis. Noticeable beats of "fast" oscillations occur with a frequency about 0.3 MG when the magnetic field makes a small angle with the c*-axis and thus within the vicinity of the principal resistance minimum. The dependence of the oscillation frequency on that angle is approximately linear when plotted in polar coordinates, whether the magnetic field is perpendicular to the b'-axis or the a-axis, those lines being perpendicular to the c*-axis and thus indicating that these oscillations are associated with an only slightly corrugated cylindrical sheet of the Fermi surface around the c*-axis. From the temperature dependence of the oscillation amplitude within the moderate temperature range, the cyclotron mass on the corresponding extremal sections of the Fermi surface can be estimated. The field dependence of the electrical resistance along the a-axis has a quasi-classical component which tends to saturate as the intensity of the magnetic field is raised, no matter how that field is oriented, and in a magnetic field almost parallel to the c*-axis it even drops somewhat when the intensity of that field is raised above 100 kOe. The authors thank N.Ye. Alekseyev and T. Palewski for support and for making the International Laboratory of Strong Magnetic Fields and Low Temperatures in Wroclaw/POLAND available, E.B. Yagubskiy and Ye.E. Laukhina for synthesizing the organic crystals, V.G. Peschanskiy and V.M. Yakovenko for fruitful discussions. Figures 13; references 24.

Critical Behavior of Multilayer Superconductors

907J0060D Moscow ZHURNAL EKSPERIMENTALNOY I TEORETICHESKOY FIZIKI in Russian Vol 97 No 4, Apr 90 pp 1371-1378

[Article by L.I. Glazman, Institute of Problems in Technology of Microelectronics and Extra-Pure Materials, and A.Ye. Koshelev, Institute of Solid-State Physics, USSR Academy of Sciences]

[Abstract] Relations for the critical properties of multilayer superconductors with weak interlayer interaction are derived in the quasi-two-dimensional approximation. The critical temperature is regarded as the measurable BCS "mean field" transition temperature, rather than the also measurable apparent zero-resistance temperature, temperature of crossover from three-dimensional to two-dimensional fluctuations, or upper bound of the fluctuation range. Inasmuch as with temperatures below the critical one, phase fluctuations of the order parameter are much more intense than its amplitude fluctuations, the latter are disregarded in the energy balance. The fluctuation width, rendered finite by even weak interlayer interaction, is determined on this basis. The temperature dependence of both longitudinal and transverse field penetration depths, and then the corresponding two critical currents, are also determined. A further concern is suppression of three-dimensional fluctuations by a magnetic field, parallel to the layers in a superconductor with sharp separation of layers and with the crossover temperature within the fluctuation range. Numerical estimates of critical temperatures and currents have been made on the basis of published experimental data pertaining to the $Bi_2Sr_2CaCu_2O_8$ material and including the Kosterlitz-Thouless temperature. The authors thank V.B. Geshkenbeyn, P. Minnhagen, D.R. Nelson, and M.V. Feygelman for discussions and helpful comments. References 27.

Anomalies of Temperature Dependence of Electrical Resistance, Critical Current, and Critical Magnetic Field Characteristic of Ba-K-Bi-O Superconductor Materials

907J0073A Moscow ZHURNAL EKSPERIMENTALNOY I TEORETICHESKOY FIZIKI in Russian Vol 97 No 5, May 90 pp 1635-1643

[Article by N.V. Anshukova, V.B. Ginodman, A.I. Golovashkin, L.N. Zherikhina, and A.M. Tskhovrebov, Institute of Physics imeni P.N. Lebedev, USSR Academy of Sciences, L.I. Ivanova and A.P. Rusakov, Moscow Institute of Steel and Alloys]

[Abstract] An experimental study of $Ba_{1-x}K_xBiO_3$ superconductor ceramics has revealed anomalies of the temperature dependence of their electrical resistance, critical current, and critical magnetic field which can all be adequately interpreted by referring to the model of a superconductor-dielectric in a spatially nonhomogeneous state, rather than to the model of a granular superconductor. The experiment was performed on three materials with x = 0.32, 0.39, 0.40 respectively, rectangular 2x5x10 mm^3 bars of ceramic having been produced by sintering $Bi_2O_3 + Ba(NO_3)_2 + KNO_3$ mixtures, first at 715°C in a nitrogen atmosphere and then at 450°C in an oxygen atmosphere followed by cooling to 150°C. Their electrical resistance was measured by the current-voltage method with a direct current and with a 23 Hz alternating current over the 300-2 K temperature range, in magnetic fields of up to 8 T intensity perpendicular to the direction of current flow and parallel to the wide edges. The anomaly in the temperature dependence of their electrical resistance is a rise along a negative slope from 300 K to 100 K followed by a plateau from 100 K to 30 K. The trend of its temperature dependence below the critical 30 K temperature depends on the magnitude of the current and on the intensity of the magnetic field. While in the absence of a magnetic field, the electrical resistance drops to zero at about 25 K, in the presence of a strong field (1.6 T) superconducting transition begins at about 20 K and ends at about 5 K when the current is small, or when the electrical resistance first continues to rise dielectric-like to a peak at about 5 K and only then drops to zero at some temperature not much lower. The anomaly in the temperature dependence of the critical current is its nonmonotonic trend with a peak at about 20 K. The current-voltage characteristic below the critical temperature includes hysteresis up to to some limiting current above which it vanishes, the hysteresis loop shrinking as the intensity of the magnetic field is raised

and the temperature is lowered. The voltage jump within this range is larger than would correspond to the energy gap in the BCS model and reversal of the current does not result in a perfectly symmetric duplication of the hysteresis loop in the third quadrant. The anomaly of the temperature dependence of the upper critical magnetic field is its positive slope, without saturation, as the temperature approaches zero. The data indicate that these ceramic materials have a multiple Josephson-junction structure. The authors thank Yu.V. Kopayev and A.A. Gorbatsevich for helpful and fruitful discussions. Figures 9; references 20.

Nuclear-Magnetic Resonance of Copper in Pr-Ce-Cu-O Superconductor

907J0074B Moscow PISMA V ZHURNAL EKSPERIMENTALNOY I TEORETICHESKOY FIZIKI in Russian Vol 51 No 11, 10 Jun 90 pp 571-574

[[Article by O.N. Bakharev, A.V. Yegorov, M.V. Yeremin, R.Sh. Zhdanov, M.S. Tagirov, and M.A. Teplov, Kazan State University]

[Abstract] Pulsed nuclear-magnetic resonance of ^{63}Cu and ^{65}Cu isotopes in $Pr_{1.85}Ce_{0.1}CuO_{4-d}$ superconductor ceramic was made, a specimen of this material having been prepared by the Tokura method. Its critical superconducting transition temperature based on magnetic susceptibility measurements was found to be 24 K and x-ray analysis revealed no extraneous phases. The specimen was ground into powder and the latter mixed with molten paraffin, whereupon a cylindrical container with this paste was placed vertically in a horizontal magnetic field of about 10 kOe intensity. Slow rotation of the heated container at a speed of 2 rpm in this magnetic field caused most of the powder grains to orient themselves along the axis of rotation and thus perpendicular to the magnetic field, owing to the anisotropy of their magnetic susceptibility. Measurements of nuclear-magnetic resonance were made at two frequencies, 8.1 MHz and 10.7 MHz, with the temperature of the specimen first 4.2 K and then 1.5 K. The duration of π-pulses and π/2- pulses was typically 7 μs and 14 μs respectively. Measurements by the spin echo method have yielded a NMR spectrum with a +0.1% paramagnetic shift and an $A(2r) = A(0)e^{-2\tau/T_2}$ decrement of the echo signal envelope in all cases. On the basis of these spectra have been calculated the widths of resonance lines and the electric field gradients, also spin-spin and spin-lattice relaxation times indicating magnetic spin-spin relaxation and most probably quadrupole relaxation respectively. The authors thank R.Yu. Abdusabirov and S.L. Korableva for assistance in preparation of the specimen. This study was a part of the No 333 project in the State "High-Temperature Superconductivity" Program supported by the Science Council for Problems of High-Temperature Superconductivity. Figures 3; tables 1; references 8.

New Phases in Organic Superconductors

907J0074C Moscow PISMA V ZHURNAL EKSPERIMENTALNOY I TEORETICHESKOY FIZIKI in Russian Vol 51 No 11, 10 Jun 90 pp 583-585

[Article by A.G. Lebed, Institute of Theoretical Physics imeni L.D. Landau, USSR Academy of Sciences]

[Abstract] A contribution to the theory of spin-density waves (SDW) is made by demonstrating analytically that transitions from one to another SDW-subphase, characteristically occurring in organic superconductor materials of the tetramethyl tetrasulfofulvalene $(TMTSF)_2X(X = ClO_4, PF_6)$, result in coexistence of several spin-density waves whose frequencies are different multiples n of the cyclotron frequency and which have different wave vectors. Included in the analysis are not only "one-dimensionalization" of the electronic spectrum in a magnetic field and instability in the Peierls, both characterizing the metal-to-SDW phase transition, but also the free energy and the second-order terms of its series expansion. The constitutional diagram is, on this basis, broken up so that new phases appear; the most significant among them being either four or eight plane waves coexisting near the critical superconducting transition temperature. Next are considered the fourth-order terms of free energy in states where the two elements Δn_0 and $\Delta\text{-}n_0^*$ in the vector-column of the order parameter are approximately equal. The author thanks L.P. Gorkov and V.M. Yakovenko for discussion and comments. Figures 1; references 11.

UDC 539.612:678.01

Mass-Spectroscopy Study of Lattice Oxygen Emission From High-T_c Superconductors Under Compressive Stress

907J0097c Leningrad FIZIKA TVERDOGO TELA in Russian Vol 32 No 5, May 90 pp 1356-1359

[Article by O. F. Pozdnyakov, V. S. Yudin, B. P. Redkov, B. T. Melekh, Engineering Physics Institute imeni A. F. Ioffe at the USSR Academy of Sciences, Leningrad]

[Abstract] Physico-chemical processes in stressed high-T_c superconductors (VTSP) were examined by the stressed state mass-spectroscopy method. The 3x5x7 mm $YBa_2Cu_3O_{7-\delta}$ and $BiSrCaCu_2O_x$ samples obtained by RF melting were uniaxially strained along the long edge in a vacuum in the immediate vicinity of the ion source of a transit time mass spectrometer. A compressive stress of 0-30 MPa was applied and measured by a strain gauge transducer. Gas emission from stressed sample was detected. The mass spectra and, consequently, composition of the volatile products developing from Y- and Ba-based VTSP are virtually the same. The analysis shows that compressed samples emit primarily molecular oxygen. Moreover, much smaller amounts of nitrogen, carbon monoxide, and probably atomic oxygen were also detected, which is typical of VTSP. Thus the

lattice oxygen loss from strained VTSP within a broad temperature range was established. References 9: 6 Russian, 3 Western; figures 4.

Niobium Nitride Superconductor Film Penetration Depth by Electromagnetic Field

907J0100B Leningrad ZHURNAL TEKHNICHESKOY FIZIKI in Russian Vol 60 No 5, May 90 pp 124-128

[Article by O. G. Vendik, A. Karpyuk, L. Kovalevich, A. B. Kozyrev, S. G. Kolesov, T. B. Samoylova, Leningrad Electrical Engineering Institute imeni V. I. Ulyanov (Lenin)]

[Abstract] Granulated NbN films with high microwave surface resistance in the normal conducting state and a relatively low surface resistance in the superconducting state are a promising material for low-noise microwave control devices and microelectronics. Their use at such frequencies is determined by the electromagnetic field penetration depth λ. The measured dependence of the resonance microwave frequency of microstrip resonators from granulated NbN films with $\rho = (1\text{-}5) \times 10^{-5}$ Ωxm on temperature is analyzed on the basis of the Ambegaokar-Baratoff model for SIS structures. The analysis of experimental data made it possible to measure the field penetration depth in thin granulated films at T_c = 11-13K. Together with Kubo, Asahi, et al. data, the results made it possible to derive the dependence of $\lambda(0)$ on $(\rho/T_c)^{1/2}$ for the values of $\rho = 5 \times 10^{-7}$ to $\rho = 5 \times 10^{-5}$ Ωxm and T_c = 11-17K. The resulting plot makes it possible to estimate $\lambda(0)$ in NbN films by simple DC resistive measurements of ρ and T_c. References 12: 5 Russian, 7 Western; figures 3; tables 1.

Frozen Photoconduction in YBaCuO Films

907J0101b Moscow PISMA V ZHURNAL EKSPERIMENTALNOY I TEORETICHESKOY FIZIKI in Russian Vol 52 No 10, 10 Jul 90 pp 696-700

[Article by A. I. Kirilyuk, N. M. Kreynes, V. I. Kudinov, Physics Problems Institute at the USSR Academy of Sciences]

[Abstract] The frozen photoconduction phenomenon was observed in the $YBa_2Cu_3O_{6+x}$ films near the metal to dielectric transition which occurs at $x = 0.45$; at lower temperatures, the film passes to the superconductor state. A subsequent increase in x leads to an increase in T_c which reaches 92K given $x = 1$. In the experiment, $YBa_2Cu_3O_7$ films on a $SrTiO_3$ 6x4 mm base produced by the laser deposition method were used. Some oxygen was removed from the film by vacuum annealing at 300°C for 10 h. It was discovered that the onset of the superconducting state occurs rather abruptly with respect to the oxygen concentration. The film was then placed in liquid helium at T = 2K and exposed to argon laser radiation at λ = 511.4 nm with a 300 μW power. The film resistance dropped sharply under exposure, but remained constant when the exposure was interrupted (i.e., the frozen photoconduction effect). Moreover, there was virtually no light-excited charge carrier relaxation in the 1.5-280K range and a wide superconductivity transition occurred below 40K in exposed films and remained for almost 20 h up to room temperature. The authors are grateful to U. I. Usoskin and V. L. Sobolev for providing the film, to A. S. Borovik-Romanov for his interest in the experiment, and to I. L. Krylov for discussing the results. References 4: 4 Western; figures 3.

The π-Phase in Laminated Magnetic Superconductors

907J0101c Moscow PISMA V ZHURNAL EKSPERIMENTALNOY I TEORETICHESKOY FIZIKI in Russian Vol 52 No 10, 10 Jul 90 pp 701-703

[Article by A. V. Andreyev, A. I. Buzdin, R. M. Ozgud, Moscow State University imeni M. V. Lomonosov]

[Abstract] A number of layered compounds can be produced today in which superconducting layers alternate with magnetic (ferro- or antiferromagnetic) layers. A model was constructed to demonstrate that the exchange interaction of conduction electrons with the magnetic layer atoms may lead to the development of a nonuniform superconducting π-phase where the parameter sign changes with the transition to the next superconducting layer. In this model, the lattice cell consists of two layers, one superconducting and one magnetic, while the quasiparticle motion is described by the same spectrum. An analysis of the model confirms that in such layered superconductors, the π-phase, in which the superconductivity order parameter changes sign with transition to the next layer, may correspond to the fundamental state of the system. References 8: 5 Russian, 3 Western; figures 1.

UDC 517.926.4

Spaces of Linear Differential Equations and Flag Manifolds

907J0011B Moscow IZVESTIYA AKADEMII NAUK SSSR: SERIYA MATEMATICHESKAYA in Russian Vol 54 No 1, Jan 90 pp 173-187

[Article by B.Z. Shapiro]

[Abstract] A linear homogeneous differential equation of n-th order $L_n[x] = x^{(n)} + a_1(t)x^{(n-1)} + ... + a_n(t)x = 0$ given on an interval I of time t with $a_i(t)$ member of set $C^{\infty}[I]$ being oscillatory or nonoscillatory on that interval I, depending on whether its nonzero solution has at least n roots or fewer than n roots; its oscillatory properties shown to be related to the behavior of a left-invariant flux it induces in the space of complete flags. Four theorems (A,B,D,F) and two corollaries (C to theorem B, E to theorem D) summarize the result of this dissertation. Following the definition of a flag curve as the transform f: I→ F_n of interval I on the manifold of complete flags F_n in the space of solutions to that equation and the definition of a general set of complete flags in the R^n space, as one where, for any set of linear subspaces belonging to different flags, the codimensionality of their intersections is equal to n or the sum of their co-dimensions, whichever is smaller. Considering that two complete flags are transversal when they form a general set or are nontransversal otherwise, the set of complete flags nontransversal to a flag α is called the loop of flag α. First are proved three lemmas pertaining to curves of differential equations and the Kartan distribution on a flag manifold. A theorem with a corollary pertaining to loops is then proved with the aid of two propositions stated without proof. A lemma is subsequently proved which establishes a criterion for a linear homogeneous differential equation being oscillatory or not, it accordingly being nonoscillatory when and only when any set of pairs of different points on its flag curve is a general one. Theorem A, which establishes the equivalence of an equation being oscillatory on the interval I = [0,1] to the flag of this equation being at some instant of time after t = 0 interval, nontransversal to its flag at time t = 0 or to the flag curve of this equation intersecting the loop of any flag, is subsequently proved in the sequence "b) implies a) implies c) implies b)" with use of the induction method on the "a) implies c)" step. The corollary C to theorem B, by virtue of theorem A, is extension of Sturm's alternation theorem to high-order linear homogeneous differential equations. With the aid of theorem A and Sherman's theorem pertaining to an ordinary linear homogeneous differential equation of n-th order, which has a solution with n or more zeros on the [0,1] half-interval, is then proved theorem D, which establishes the boundary of the range of nonoscillatory equations and, as corollary E, diffeomorphism of singularities on that boundary and singularities on intersections of the loop of the initial flag of the flag curve for that equation. Following a proof of theorem F pertaining to these singularities, theorem D is proved again, but topologically, with the aid of two lemmas which pertain to hyperplane intersecting the germ of a non-planar curve. Figures 1; references 21.

UDC 62-50

Fuzzy Differential Inclusions

907J0018A Moscow PRIKLADNAYA MATEMATIKA I MEKHANIKA in Russian Vol 54 No 1, Jan 90 pp 12-17

[Article by V.A. Baydosov (deceased), Sverdlovsk]

[Abstract] Differential equations are considered, in which some of the parameters are exactly unknown, but some information about their preferred values is given. A differential inclusion with a fuzzy right-hand side is defined as a formal symbolic relation in accordance with the theory of fuzzy sets, whereupon a fuzzy set of solutions to such a differential inclusion, and then a proper fuzzy set are defined. First is established, by proof, the necessary and sufficient condition for function x(.) to be the solution to an ordinary differential inclusion. It is also demonstrated that for a proper fuzzy set A, there exists a max [begin set with]a: A_a not an empty set [end set]. Next is established the necessary and sufficient condition for a multivalued transform of a proper fuzzy set $\Psi_a(t,x)$ to be semicontinuous from above, with respect to (t,x), its validity proven by reductio ad absurdum. Next comes a differential inclusion with a fuzzy right-hand side generated by a differential equation $\dot{x} = f(t,x,k(t))$ with a vector of parameters (coefficients) k(t) in space R^r and with (t,x) in space G. Three theorems are proven for such a differential inclusion. The first one establishes the equality $f_a(t,x,K(t)) = f(t,x,K_a(t))$ when $a > 0$ for a proper fuzzy set K(t) and function f(x,t,k) continuous in k, with two corollaries. The second one establishes the necessary and sufficient condition for semicontinuity of the transform K_a, with a corollary. The third one establishes that there is a $d > 0$ for which there exists a non-empty set of solutions satisfying the initial condition $x(t_0) = x_0$. Differential inclusions with a right-hand side measurable in time t are considered last, a theorem proven which establishes when the right-hand side is measurable. References 6.

UDC 517.5

Optimal Recovery of Differentiable Functions

907J0021A Moscow MATEMATICHESKIY SBORNIK in Russian Vol 181 No 3, Mar 90 pp 334-353

[Article by B.D. Boyanov, Sofia University/Bulgaria/]

[Abstract] The problem is to optimally recover function f from a class of smooth functions M, defined on the

interval I = [0,1] on the basis of known T(f) = (l_1(f),...,l_nN(f), where [begin set with] l_i [end set] are linear functionals defined in class M. The problem is analyzed and solved for the class of functions $W_{\infty,\sigma}^{L}$(I) = [begin set with] f member of set L_∞^r(I)||Lf(x)|| = or < σ(x) for all x on I [end set] where the operators L are L(y) = ($1/w_r$(d/dx $1/w_{r-1}$(d/dx...($1/w_1$d/dx y/w_0...)), w_k(.) member of set C^{r-k}(I) and $w_k(x) > 0$ for all x on I. Assuming that an identity matrix satisfies the Atkinson-Sharma condition, a resolvable identity matrix is defined in terms of a nonsingular one. With an L-spline and a complete L-spline also having been defined, five relevant theorems are stated and then proved. The first three of them are Favara's theorem, the existence and uniqueness theorem for interpolation splines, and the recovery theorem for class $W_{\infty,\sigma}^{L}$(I)functions stating that the interpolation method is the best one of recovering one on the basis of known [begin set with] $L_j f(\xi_i)$||e_{ij} = 1 [end set]. For proving these three theorems, the generalized Rolle's theorem, the integral representation theorem, Borsuk's theorem, and the duality theorem for recovery may all be used. The fourth theorem, which establishes the existence and uniqueness of an L_{gs}-spline with N-r nodes when $\nu_1,...,\nu_n$ are natural numbers ranging from 1 to r and $\Sigma\,\nu_k$ (k from 1 to n) = N = or > r, is proved with the aid of five lemmas. The fifth theorem establishes the existence and uniqueness of a set of nodes (all ε_k)$_1^n$ when the differential L- operator has the property that w_0(x) is identically equal to 1 and $\nu_1,...,\nu_n$ are natural numbers from 1 to r, is proven by reductio ad absurdum. There follows a comparison (inequality) theorem for w_0, not identically equal to 1, with a corollary for every set of numbers (ν_k)$_1^n$ as defined. Periodic differentiable functions are treated separately, but in terms of analogs and by only indicating the modifications necessary for proving those five theorems for this case. The author thanks V.M. Tikhomirov for assistance. References 27.

UDC 517.95

Dependence of Solutions to Boundary-Value Problems on Vector-Field Perturbation of Their Domain

907J0021B Moscow MATEMATICHESKIY ZHURNAL in Russian Vol 181 No 3, Mar 90 pp 367-38

[Article by A.K. Kerimov, Institute of Terrestrial Magnetism, Ionosphere, and Radio Wave Propagation, USSR Academy of Sciences, Troitsk]

[Abstract] Growth of solutions to boundary-value problems in Holder norms for the Poisson equation, due to vector-field perturbation of their domain, is estimated on the basis of two theorems pertaining to a set of vector fields V_δ, with two constants C_1,C_2 satisfying certain inequalities with a lower bound and an upper bound respectively, in a domain whose free boundary $\delta\Omega_0$ is a surface of the $C^{l+\gamma}$ class. Both theorems are proven with the aid of three lemmas, whereupon two auxiliary estimates are validated. This is followed by parametrization of domains which involves derivatives with respect to vector fields, on the basis of a proposition and also a third theorem proven with the aid of a lemma. A fourth theorem is proven next, with the aid of that proposition, that last lemma, and the first theorem, which then validates priori estimates in analysis of the Poisson equation in the form $\varphi(\alpha,\upsilon) = (\gamma^2 + |\Delta u(\alpha,\upsilon)|^2)_S$. Figures 3; references 11.

UDC 530.16

Lyapunov Instantaneous Exponents

907J0027 Kiev DOKLADY AKADEMII NAUK UKRAINSKOY SSR, SERIYA A: FIZIKO-MATEMATICHESKIYE NAUKI in Russian No 2, Feb 90 pp 50-52

[Article by D.M. Vavriv and V.B. Ryabov, Institute of Radio Astronomy, UkSSR Academy of Sciences, Kharkov]

[Abstract] Evolution and structure of a strange attractor are considered, Lyapunov instantaneous exponents introduced for a full description of its local properties. These exponents are obtained from a system of ordinary differential equations x = F(x,t) (x in set of real numbers R^n) describing a dynamical system and from the corresponding linearized system of equations yielding the evolution of an arbitrary vector y in a tangent space dy/dt = J(x,t)y where J(x,t) = partial derivative of F(x,t) with respect to x. As the spectrum of Lyapunov instantaneous exponents μ_k(t) (k = 1,2,...,n) are regarded as the logarithmic time derivatives of the norms of arbitrary orthogonal vectors [begin set with] y_k [end set](t) in that tangent space. For an analysis of dynamical systems, the Lyapunov characteristic exponents λ_k are obtained from the corresponding Lyapunov instantaneous exponents μ_k by averaging the latter over the time period T of attractor motion. In the case of an ergodic process $\lambda_k = \lim(T \to \infty)$ integral of μ_k(t) from t = 0 to t = T so that each Lyapunov characteristic exponent λ_k is the first initial moment of the probability distribution of the corresponding Lyapunov instantaneous exponent μ_k. Calculating the spectrum of Lyapunov characteristic exponents becomes simple, which is demonstrated on an arbitrary nonautonomous system of two second-order differential equations $dx_1/dt = f_1(x_1,x_2,t)$ and $dx_2/dt = f_2(x_1,x_2,t)$. From the corresponding system of two equations for both amplitude A and phase Φ of the vector in the tangent space, where $f_{ij} = \delta f_i/\delta x_j(t)$, is obtained, an expression for the Lyapunov instantaneous exponents $\mu_{1,2}$ in terms of sin2Φ and cos2Φ. The general conditions for onset of random oscillations can be established directly from the

Lyapunov instantaneous exponents, which is demonstrated on a passive oscillator with a weak, approximately cubic nonlinearity and quasi-periodic external excitation. References 11.

UDC 517.956.32

Dirichlet Problem and Nonlocal Boundary-Value Problems for Wave Equation

907J0030A Minsk DIFFERENTSIALNYYE URAVNENIYA in Russian Vol 26 No 1, Jan 90 pp 60-65

[Article by T.Sh. Kalmenov and M.A. Sadybekov, Kazakh State University imeni S.M. Kirov]

[Abstract] A variant of the Dirichlet problem for the two-dimensional nonhomogeneous wave equation $Lu = u_{xx}-u_{yy} = f(x,y)$ is analyzed for solvability and for smoothness of the solution. Along with the Dirichlet problem, finding a solution which will satisfy the condition $u|_{AB \cup AC \cup BC} = 0$ is also considered, and the Darboux problem, finding a solution which will satisfy the condition $u|_{AB \cup AC} = 0$. A theorem is stated which not only establishes the existence and uniqueness of a strong solution u member of set $W_2^1(\Omega)$ to the Darboux problem with any f(x,y) member of set $L_2(\Omega)$, but also provides an estimate with an upper bound for the norm of this solution. The general solution $\varphi(x)$ to a functional equation $\varphi(x) = \varphi(a(x))$ for x from 0 to 1 having been obtained next, an existence and uniqueness theorem for a quasi-regular solution and for a semi-strong solution to the Dirichlet problem is proved with the aid of a lemma and a corollary to the latter. Another theorem is then proved stating that the closure L_+ on $L_2(\Omega)$ in the Darboux problem is the conjugate of closure L in $L_2(\Omega)$ in the Dirichlet problem. A corollary to this theorem is that this Dirichlet problem is a Volterra boundary-value problem in the sense of the inverse operator L^{-1} being a completely continuous nilpotent one on $L_2(\Omega)$. Inasmuch as the solution to this Dirichlet problem is not continuous at point A, according to the solvability theorem for this problem, the following nonlocal problem S_α for function α in the same class C is considered: to find a solution u to that given wave equation which will satisfy, not only the Dirichlet condition, but also the condition $\alpha u((\tau))+(1-\alpha)\lim u(\mathrm{Theta}_k(\tau))(k \to \infty) = 0$ where $\mathrm{Theta}_k(\tau)$ is the point of intersection of characteristics $x - y = a_k(1)$ and $x + y = a_k(\tau)$. An existence and uniqueness theorem for a quasi-regular solution to this problem is proved with the aid of a lemma involving Hilbert-Schmidt operators, a corollary to this theorem being that such a problem S_α is a Volterra boundary problem if, and only if, $\alpha(1 - \alpha) = 0$. References 11.

UDC 517.95

Cauchy Problem for Indeterminate Systems of Linear Differential Equations

907J0030B Minsk DIFFERENTSIALNYYE URAVNENIYA in Russian Vol 26 No 1, Jan 90 pp 75-85

[Article by M.V. Korovina, Moscow State University imeni M.V. Lomonosov]

[Abstract] Following the definition of flag N on a complex-analytic n-dimensional manifold M and of a vector-space J_N^p of jets on flag N, the Cauchy problem is formulated for a system of linear differential equations $F(j^n(u(x))) = f(x)$ involving a holomorphic function u(x) and a vector-column f(x) of length l equal to the number of equations in the system. The linear operator $F:J^n \to C^l$ in each layer J_x^n of the jet J^n depends holomorpically on point x of manifold M, corresponding to an (lxp)-dimensional matrix where p denotes the number of all derivatives of orders up to and including n. Additional constraints on function u(x) lead to the problem $F(j^{n-N}p(u(x)) = v$ where v is an element of vector-space J_N^p. The matrix of that system of equations is assumed to be of a rank lower than or equal to n. A finite-dimensional factor-space $J_{m,NS,\ldots N_1}{}^{n,p}{}_{S,\ldots,p_1}$ is then introduced, for solution of the Cauchy problem on flag N. An existence and uniqueness theorem is proven for a solution to that problem, if the latter is solvable in series and F is an isomorphism. It is proved for n = 1 only, the proofs for higher n being analogous. In search of a formal solution to this Cauchy problem for a system of linear differential equations with constant coefficients, a theorem is subsequently proved stating that on every manifold N_i (i = 1,...,s), there exists a finite system of differential operators $Q_j{}^i$ (j = 1,...,m) such that the conditions $Q_j{}^i\tilde{v}^{(i)}$ are the necessary and sufficient ones for this problem to have a formal solution. A simple example is then considered in the Cauchy problem on a system of two embedded manifolds F = [begin set with]N_1 contained in N_2[end set]. The author thanks V.A. Ilin, B.Yu. Sternin, and V.Ye. Shatalov for assistance in formulation of the problem and subsequent cooperation. References 5.

UDC 517.9

Necessary and Sufficient Conditions for Topological Equivalence of Three-Dimensional Dynamic Morse-Smale Systems With Finite Number of Singular Trajectories

907J0035A Moscow MATEMATICHESKIY SBORNIK in Russian Vol 181 No 2, Feb 90 pp 212-239

[Article by Ya.L. Umanskiy, Gorkiy Institute of Agriculture]

[Abstract] A complete topological invariant is constructed for three-dimensional dynamic Morse-Smale systems with a finite number of singular trajectories along with closed ones (orbits). Following the definition of a C^2- smooth dynamic Morse-Smale system X on an orientable and oriented smooth, closed and connected manifold M, singular trajectories of system X are defined as non-wandering trajectories which belong in one-dimensional invariant manifolds of saddle equilibrium states and those which belong in intersection of two-dimensional invariant manifolds of non-wandering saddle trajectories. It is demonstrated that a dynamic Morse-Smale system has a finite number of singular trajectories when, and only when, at least one invariant manifold of any closed saddle trajectory L, if one exists, does not contain singular trajectories other than this one. A homeomorphism theorem is then proved, whereupon two lemmas are proved pertaining to sheaves of separatrices and to cells of such a dynamic system respectively, four kinds of cell are identified. After a ω-scheme of a cell boundary has been defined as the list of traces of sheaves and a ω-scheme of system X (arrangement of cells) has been defined as the totality of the ω boundary schemes of all cells with indication of source and sink for each cell. An α-scheme of system X being defined analogously, a lemma is proved stating that the ω-scheme of system X and the α-scheme of system X determine each other uniquely. Next, the equivalence of schemes is considered, which leads to the fundamental theorem stating that dynamic Morse-Smale systems with a finite number of singular trajectories given on three-dimensional smooth oriented manifolds are topologically equivalent when, and only when, their schemes are equivalent. After first, the necessity, and then, the sufficiency of the conditions for this theorem have been established, a procedure is outlined for construction of a homeomorphism which conjugates two such system X and X'. Figures 4; references 18.

UDC 519.2

Averaging Principle for Systems of Stochastic Differential Equations

907J0035B Moscow MATEMATICHESKIY SBORNIK in Russian Vol 181 No 2, Feb 90 pp 256-268

[Article by A.Yu. Veretennikov, Institute of Control Problems]

[Abstract] The averaging principle is applied to a system of stochastic differential equations on the basis of three validating theorems. The first theorem establishes weak convergence of the solution within any time $T > 0$ as the parameter $\varepsilon \to 0$, when five inequalities, which include the Lipschitz condition, are satisfied. The second theorem then establishes existence of a limit to which the solution converges, this limit being the unique solution to the Cauchy problem for such a system of equations. The third theorem establishes convergence of the solution in terms of probability, namely that the probability of the deviation from the solution being larger than some arbitrary δ within some time, not longer than T, is zero as $\varepsilon \to 0$. Each theorem is proved. The author thanks R.Ya. Chitashvili and V.V. Yurinskiy for helpful comments. References 15.

UDC 517.944

New Mathematical Model of Heat Conduction Processes

907J0036A Kiev UKRAINSKIY MATEMATICHESKIY ZHURNAL in Russian Vol 42 No 2, Feb 90 pp 237-245

[Article by V.I. Fushchich, A.S. Galitsyn, and A.S. Polubinskiy, Institute of Mathematics, UkSSR Academy of Sciences, Kiev]

[Abstract] A new equation, a fourth-order partial differential one invariant with respect to the Galilean group, is proposed for a description of thermal and diffusion processes. With the process parameters definitively given, this mathematical model is not only more adequate than the classical linear equation of the parabolic kind, but is also suitable for analysis of special cases. The equation Lu identically equal to $\alpha_1 L_1 u + \alpha_2 L_2 u = 0$ ($L_2 = L_1 L_1$), a biparabolic equation of heat conduction is derived from the equation of energy conservation $\delta e/\delta t = \text{div } q \text{ (vector)} = 0$, with energy e and thermal flux q expressed by corresponding field equations. The fundamental solution to this equation, or to operator L, is a generalized function of the Galilean group G which makes the left-hand side equal, not to zero, but to $4\pi\delta(\text{vector } R)\delta(\tau)$. The integral representation of the solution to a boundary-value problem for this equation is obtained by considering the nonhomogeneous equation $Lu(x,t) = f(x,t)$, whereupon the boundary conditions for the one-dimensional Cauchy problem and the initial

conditions for the operator L are stipulated. Solutions of the traveling-wave kind are obtained first, then solutions for a power-law boundary condition $u(0,t) = (1 + t)^{\alpha}$ (constant $\alpha > 0$) and for a power-law condition with peaking $u(0,t) = (T - t)^{-\alpha}$ (constant $\alpha > 0$). References 10.

UDC 519.21

Lower Bounds for Tails in Distributions of Certain Functions of Normally Distributed Random Quantities

907J0051C Moscow DOKLADY AKADEMII NAUK SSSR in Russian Vol 311 No 3, Mar 90 pp 521-523

[Article by E.B. Bagirov, Institute of Mathematics imeni V.A. Steklov, USSR Academy of Sciences, Moscow]

[Abstract] The lower bounds are obtained for estimation of tails in distributions of a random quantity $Q = \Sigma \lambda_j(Z_j + a_j)^n$ over j from 1 to N (n and N are natural numbers, λ_j and a_j are any real number, and Z_j are mutually independent random quantities normally distributed over the [0,1] interval), this quantity having been normalized to its mean value and standard deviation. The lower bound is defined by the inequality P[begin set with]$V = \text{or} > x$[end set] = or $> 1 - \Phi(xp_V(0)/1(2\pi)^{-1/2})$ for the density of Q "at zero" and is best estimated in terms of a characteristic function for each specific case. Two theorems, proved with the aid of two lemmas, validate two inequalities for any n = 2,3,... and x 0 reading of Q. A third lemma pertains to the values of constants γ_n in the expressions for the coefficients of the distribution tails. Article was presented by Academician Yu.V. Prokhorov. References 5.

UDC 515.1

Spectral Estimates of Compact Pseudodifferential Operators on Nonlimited Sets

907J0107a Moscow MATEMATICHESKIY SBORNIK in Russian Vol 181 No 7, Jul 90 pp 995-1006

[Article by A. S. Andreyev, Naval Radio Engineering School imeni A. S. Popov, Leningrad]

[Abstract] The spectrum of compact matric pseudodifferential operators on a nonlimited set is investigated in a Euclidean space. The set boundary smoothness condition coincides locally with the corresponding conditions. The pseudodifferential operator symbol is assumed to be a smooth matrix-function. No assumption is made regarding the fixed signs or constant multiplicity of the matrix-symbol's eigenvalue. The operator spectrum is estimated by the variational method. The proof rests primarily on local results. Under additional symbol behavior regularity conditions, these estimates identify the spectrum's asymptotics and the order of the remainder term. The author is grateful to M. Z. Solomyak for useful discussions. References 6: 4 Russian, 2 Western.

END OF FICHE DATE FILMED

11 January 1991